

SLAC-PUB-3224

October 1983

T/E

**APPLICATION OF A SOFTLY BROKEN SUPERSYMMETRIC MODEL
TO THE PROPERTIES OF THE SCALAR NEUTRINO***

HOWARD E. HABER

Department of Physics

*University of California, Santa Cruz, California 95064***

and

Stanford Linear Accelerator Center

Stanford University, Stanford, California 94305

R. MICHAEL BARNETT

Institute for Theoretical Physics

University of California, Santa Barbara, California 93106

KLAUS S. LACKNER***

Stanford Linear Accelerator Center

Stanford University, Stanford, California 94305

Submitted to Physical Review D

*Work supported in part by the Department of Energy contract number DE-AC03-76SF00515.

**Permanent address.

***Address as of October 4, 1983: Los Alamos National Laboratory, Los Alamos, New Mexico 87545.

ABSTRACT

We describe a simple, softly broken supersymmetric model of electroweak interactions. In its simplest form, supersymmetry breaking is imposed via explicit mass terms for scalar quarks and leptons. We apply this model to the discussion of the decay properties of the scalar neutrino, ν_s . The one-loop process $\nu_s \rightarrow \nu + \tilde{\gamma}$ ($\tilde{\gamma} = \text{photino}$) is computed as well as multi-body (tree-level) decays of the ν_s . The relative branching ratios are crucial for determining the phenomenological signatures of the scalar neutrino. Complications to the model due to Majorana mass terms for the gauge fermions are discussed. Explicit Feynman rules for the model are listed.

1. Introduction

All high energy physics experiments seem to be consistent with what is known as “the standard model”.¹ This model describes particle physics by an $SU(3) \times SU(2) \times U(1)$ gauge theory which is spontaneously broken down to $SU(3) \times U(1)$ at a scale of roughly 300 GeV. Many models have been made which unify the standard model into one grand-unifying gauge group² (e.g. $SU(5)$). All such attempts have the unpleasant feature that the grand unification scale is at least a factor of 10^{12} larger than the scale of weak interaction. The appearance of such a large dimensionless number is known as the hierarchy problem.³ A related problem called the naturalness problem⁴ is slightly more technical; it occurs due to the existence of elementary scalar fields required to initiate spontaneous $SU(2) \times U(1)$ symmetry breaking. The masses of these scalars must be orders of magnitude less than the grand-unified scale; this is highly “unnatural”. Due to the scalar particles, the unrenormalized theory contains quadratic divergences. As a result, the tree-level hierarchy is unstable under quantum corrections. One has to fine-tune the parameters of the scalar potential to very high order in perturbation theory to insure the required hierarchy of scales.

Supersymmetric theories have been proposed as a possible solution to the problems described above.⁵ In such theories, the existence of elementary scalar particles is required by the underlying supersymmetry. Furthermore, there exists a scalar partner for each presently-known fermion. If supersymmetry is relevant to the solution of the hierarchy and naturalness problems, then the masses of supersymmetric partners of known particles cannot be much larger than 1 TeV. Furthermore, various supersymmetric models allow for the existence of much lighter supersymmetric particles, some of which may already be accessible to

accelerators either presently running or soon to be built. Thus, one way to test supersymmetric models experimentally is to search for new scalar particles. However, it has been a major disappointment that absolutely no experimental evidence for or against supersymmetry has been found.⁶ Therefore, it is essential to seek further means for determining whether supersymmetry is relevant and which classes of models are indicated.⁷

In general, for a given fermion f there are two complex scalar fields which we will henceforth denote as f_{sL} and f_{sR} .⁸ However, if right-handed neutrinos do not exist (or are extremely massive with $m_{\nu_R} \gg 300 \text{ GeV}$), then there is only one scalar neutrino relevant for low energy physics. Supersymmetry also leads to fermionic partners for both spin 1 (gauge) bosons and spin 0 (Higgs) bosons. The physical mass eigenstates are model dependent; they typically mix various combinations of two-component fermion fields into charged Dirac four-component fermions and neutral Majorana fermions.⁹ We illustrate these features by constructing a simple softly broken supersymmetric model of electroweak interactions in Section 2. This is accomplished in two steps—first an unbroken supersymmetric $SU(2) \times U(1)$ model is constructed where the gauge symmetry spontaneously breaks at tree level to $U(1)_{EM}$. Supersymmetry is then broken by adding explicit supersymmetric breaking terms. These terms are chosen to be soft, i.e. they do not add new quadratic divergences to the unrenormalized theory. The simplest set of terms one can add are explicit masses for scalar quarks and leptons. Feynman rules for the resulting model are listed in Appendix A.

Experimental searches have already been made at PEP and PETRA for charged scalar leptons and scalar quarks.¹⁰ Their results set lower limits for the masses of such objects. For example, assuming the photino is massless, the

MAC and MARK II groups state a lower limit on the scalar electron mass to be about 21-24 GeV. The limits on the scalar muon and tau leptons from MARK-J are 18 GeV and 16.5 GeV respectively. Limits on scalar quarks are harder to come by and more model dependent. If the decay $\bar{q}_s \rightarrow q + \tilde{\gamma}$ were dominant (and $m_{\tilde{\gamma}} \approx 0$), then the lower limits on the scalar quark masses are 15-16 GeV.

As for the scalar neutrino, the only known experimental bounds can be deduced from the non-observation of anomalous τ -decays.¹¹ From this, we ascertain the non-existence of the decay $\tau^- \rightarrow \nu_{s\tau} e^- \nu_{se}$ which roughly implies that $M_{\nu_{s\tau}} + M_{\nu_{se}} \gtrsim m_\tau$ (depending on the size of the wino mass). In order to search experimentally for evidence of the scalar neutrino, one needs to know its decay modes and branching ratios. The calculation of these modes has already been summarized by us in a previous paper.¹² In Sections 3 and 4 we present the calculation for two-body and multi-body decays of the scalar neutrino using the model described above (and in Section 2).

The model which we shall discuss in Section 2 is certainly a minimal one. However, we argue that the results obtained are not likely to change much in more complicated versions. In order to illustrate some of the complications that may occur, we study in Section 5 how the model changes by the introduction of Majorana mass terms for the gauginos. This introduces non-trivial mass matrices in the gaugino-higgsino sector and new mass eigenstates which are different linear combinations of the gauginos and higgsinos. As a result, new Feynman rules for these particles are needed and are discussed in Appendix B.

Section 6 contains our conclusions. We have provided two further appendices (C and D) which provide useful details needed for the computation of scalar-neutrino decay rates.

2. A Softly Broken Supersymmetric $SU(2) \times U(1)$ Model

In order to make a phenomenological study of various processes involving new supersymmetric particles, it is necessary to make use of some model. At the same time, it is desirable to proceed in a fashion as “model-independent” as possible. We have chosen to use a softly broken supersymmetric $SU(2) \times U(1)$ model which is described in this section. There are a number of reasons why we did not use a spontaneously broken supersymmetric $SU(2) \times U(1)$ model. First, it is well known among model builders¹³ that it is difficult to build a compelling spontaneously broken supersymmetric model which at low energies resembles the standard model. Second, there has been much recent work in supergravity,^{14–16} which shows that the effective low energy theory of a spontaneously broken supergravity coupled to matter fields is simply a globally supersymmetric theory broken by various soft terms.¹⁴

In constructing a softly broken supersymmetric model, we shall start from an unbroken (globally) supersymmetric theory and add to it all possible soft supersymmetry-breaking terms (following the rules of Girardello and Grisaru¹⁷). This would almost be a “model-independent” procedure, in that one would then require experiment to determine all unknown coefficients of the newly added terms. Unfortunately this procedure is too general (without any prior experimental information) and theoretical predictions depend on too many parameters. We propose to be less general at the beginning by first constructing an unbroken supersymmetric version of the $SU(2) \times U(1)$ model of electroweak interactions. We then add (at first) only those soft supersymmetry breaking terms necessary to avoid conflict with experiment. Specifically, we will only add mass terms for the scalar quarks and leptons (and for the gluinos). This allows us to make

predictions for various supersymmetric processes which depend only on a few unknown masses. It is important to consider how such predictions change if the set of soft supersymmetry breaking terms is more complicated. In Section 5, we briefly study the effect of a more complicated gaugino-higgsino mass matrix.

As for the unbroken supersymmetric versions of $SU(2) \times U(1)$, we first introduce the minimal number of fields necessary to break the gauge symmetry down at tree level to $U(1)_{EM}$ and give masses to the quarks and leptons. This requires two $SU(2)$ doublet chiral Higgs superfields and one $SU(2) \times U(1)$ singlet chiral Higgs superfield. We note that Fayet¹⁸ first wrote down a supersymmetric $SU(2) \times U(1)$ model whose chiral multiplets were exactly those mentioned above. However, Fayet¹⁸ originally attempted to interpret those multiplets as ones which contain the leptons along with the Higgs.¹⁹ We shall maintain a strict separation and add separate chiral superfields which contain the ordinary leptons (and quarks).²⁰ This is necessary, because if the scalar partner of the neutrino gains a vacuum expectation value, it will spontaneously break lepton number.²¹

Our model consists of the superfields listed in Table 1. Our notation is as follows.²² For gauge multiplets (in the Wess-Zumino gauge), we denote $V = (V_\mu, \lambda, D)$ where V_μ is the gauge field, λ is the gaugino, and D is an auxiliary scalar field. For chiral multiplets, we denote $S = (A_S, \psi_S, F_S)$ where A_S is the scalar partner of the fermion ψ_S and F_S is an auxiliary scalar field. The Lagrangian for the model is obtained in the standard fashion.²³ All we need to provide is the superpotential:

$$W = h\epsilon_{ij}T^iS^jN + sN + W_F \quad (1)$$

where i, j are $SU(2)$ indices and W_F contains terms which are responsible for

quark and lepton masses:

$$W_F = \epsilon_{ij} \left[f_{ab} T^i L_a^j R_b + h_{ab} T^i Q_a^j D_b + \tilde{h}_{ab} S^i Q_a^j U_b \right] \quad (2)$$

The Yukawa couplings f_{ab} , h_{ab} , and \tilde{h}_{ab} are related to quark and lepton mass matrices. With the possible exception of the t -quark, these Yukawa couplings are small and we will neglect them for the remainder of the paper. The scalar potential, V , is obtained from

$$V = \sum_k \left| \frac{\partial W[A]}{\partial A_k} \right|^2 + \frac{1}{2} g^2 \sum_a \sum_a (A^* T^a A)^2 + \frac{1}{2} g'^2 \sum_k (y_k A_k^+ A_k)^2 \quad (3)$$

In eq. (3), $W[A]$ is obtained from W given in eq. 1 by replacing the superfields by their corresponding component scalar fields (denoted collectively here by A_k). In the second term in eq. 3, the first (unlabeled) summation represents a sum over all SU(2) multiplets of scalar fields (in our model, the sum is over SU(2) doublets); T^a are the corresponding generators in the appropriate representation. In the third term of eq. 3, $Y_k = 2y_k$ are the U(1) hypercharges of the A_k . It is then straightforward to compute the scalar (Higgs) potential. The potential has a minimum when

$$\begin{aligned} \langle A_S \rangle &= \frac{1}{\sqrt{2}} F \begin{pmatrix} 0 \\ 1 \end{pmatrix} \\ \langle A_T \rangle &= \frac{1}{\sqrt{2}} F \begin{pmatrix} 1 \\ 0 \end{pmatrix} \end{aligned} \quad (4)$$

and all other scalar fields having zero vacuum expectation values.²⁴ The constant F is related to h and s of eq. 1 by $\frac{1}{2} F^2 h + s = 0$. It is easy to see that at this minimum, $V = 0$, thus implying that the theory remains supersymmetric. —Equation 4 indicates that $SU(2)_W \times U(1)_Y$ has broken down to $U(1)_{EM}$. We will momentarily add explicit scalar mass terms for the scalar quarks and leptons

(which are massless in the approximation that W_F given by eq. 2 is neglected). First however, let us study the supersymmetry theory of broken $SU(2)_W \times U(1)_Y$.

Some of the supersymmetric multiplets listed in Table 1 must get rearranged (in a supersymmetric way) to reflect the fact that the W^\pm and Z^0 gauge bosons get mass via the Higgs mechanism. The simplest way to see the results of this rearrangement is to first compute the fermion mass matrix which couples higgsinos and gauginos. This mass matrix arises because of the coupling $\lambda\psi A$ which occurs in supersymmetry; when A gains a vacuum expectation value, this results in a fermion mass term. In the model described here, we find the following fermion mass terms (using two-component notation for the fermion fields):

$$\begin{aligned}
& -iF\left(\frac{g^2 + g'^2}{2}\right)^{1/2} \lambda_z \left(\frac{\psi_{S_2} - \psi_{T_1}}{\sqrt{2}}\right) + Fh \psi_N \left(\frac{\psi_{S_2} + \psi_{T_1}}{\sqrt{2}}\right) \\
& + \frac{iFg}{\sqrt{2}}(\lambda^- \psi_{S_1} + \lambda^+ \psi_{T_2}) + \text{h.c.}
\end{aligned} \tag{5}$$

where $\lambda^\pm = \frac{1}{\sqrt{2}}(\lambda^1 \mp i\lambda^2)$, $\lambda_z = (g\lambda^3 - g'\lambda')/\sqrt{g^2 + g'^2}$ and the subscripts 1,2 are $SU(2)_W$ indices. By computing the vector boson mass matrix, one learns that $m_W^2 = \frac{1}{2}g^2F^2$ and $m_Z^2 = \frac{1}{2}(g^2 + g'^2)F^2$. This implies that the following four-component Dirac fermions exist in the spectrum:

$$\omega_1^- = \begin{pmatrix} \psi_{T_2} \\ i\bar{\lambda}^+ \end{pmatrix}, \quad \omega_2^+ = \begin{pmatrix} \psi_{T_2} \\ i\bar{\lambda}^- \end{pmatrix} \quad \text{with mass } m_W \tag{6}$$

$$\tilde{z} = \begin{pmatrix} (\psi_{T_1} - \psi_{S_2})/\sqrt{2} \\ i\bar{\lambda}_z \end{pmatrix} \quad \text{with mass } m_Z \tag{7}$$

$$\tilde{h} = \begin{pmatrix} (\psi_{S_2} + \psi_{T_1})/\sqrt{2} \\ \bar{\psi}_N \end{pmatrix} \quad \text{with mass } m_h \equiv hF \tag{8}$$

Finally, there is a photino $\lambda_\gamma = (g'\lambda^3 + g\lambda')/\sqrt{g^2 + g'^2}$ which remains massless.

The final step is to compute the scalar masses. One finds

$$\begin{aligned} H^+ &= \frac{1}{\sqrt{2}}(A_{S_1} + A_{T_2}^*) && \text{with mass } m_W \\ H^0 &= \text{Re}(A_{T_1} - A_{S_2}) && \text{with mass } m_Z \end{aligned} \quad (9)$$

and four mass degenerate scalar fields:

$$\begin{aligned} h_1^0 &= \text{Re}(A_{S_2} + A_{T_1}) \\ h_2^0 &= \text{Im}(A_{T_1} - A_{S_2}) && \text{with mass } m_h \\ h_3^0 &= \text{Re } A_N \\ h_4^0 &= \text{Im } A_N \end{aligned} \quad (10)$$

Thus, the new supersymmetric multiplets consists of a massless gauge multiplet $(\tilde{\gamma}, \gamma)$, three massive vector multiplets: (H^-, ω_1^-, W^-) , (H^+, ω_2^+, W^+) and (H^0, \tilde{z}^0, Z^0) and a massive chiral multiplet: (h_i, \tilde{h}) ($i = 1, \dots, 4$). Note that each multiplet has equal numbers of fermionic and bosonic degrees of freedom.

The photino $\tilde{\gamma}$ is a four-component Majorana spinor of the form:

$$\tilde{\gamma} = \begin{pmatrix} -i\lambda_\gamma \\ i\bar{\lambda}_\gamma \end{pmatrix} \quad (11)$$

By comparison, \tilde{z}^0 is a four-component Dirac spinor (see eq. 7). In fact, the existence of such an object is very special to the model considered so far. Hence, it will be useful to rewrite \tilde{z}^0 in terms of the two mass degenerate four-component Majorana spinors. We will find later that these two fermions will be split in mass in more general circumstances, for example, when an explicit Majorana gaugino mass terms is added.

Let us define:

$$\psi_1 = \frac{-i\lambda_z + \psi}{\sqrt{2}} \quad (12)$$

$$i\psi_2 = \frac{-i\lambda_z - \psi}{\sqrt{2}} \quad (13)$$

where

$$\psi \equiv \frac{\psi_{T_1} - \psi_{S_2}}{\sqrt{2}}. \quad (14)$$

It then follows that the mass terms become:

$$m_Z(i\lambda_z\psi - i\bar{\lambda}_z\bar{\psi}) = \frac{-m_Z}{2}(\psi_1\psi_1 + \bar{\psi}_1\bar{\psi}_1 + \psi_2\psi_2 + \bar{\psi}_2\bar{\psi}_2) \quad (15)$$

which allows us to identify two Majorana spinors \tilde{z}_1 and \tilde{z}_2 :

$$\tilde{z}_1 = \begin{pmatrix} \psi_1 \\ \bar{\psi}_1 \end{pmatrix}, \quad \tilde{z}_2 = \begin{pmatrix} \psi_2 \\ \bar{\psi}_2 \end{pmatrix}. \quad (16)$$

Note the factor of i in eq. 13; this insures that the fermion mass eigenvalue is positive.

The Feynman rules for the model are obtained by the straightforward but tedious procedure of expressing all fields in the supersymmetric Lagrangian in terms of physical fields thereby obtaining all interaction terms of interest. When we next add soft supersymmetry breaking consisting *only* of scalar mass terms, there are no changes in rules obtained. A list of rules that were required for our computations are given in Appendix A. However, adding additional soft supersymmetry breaking can indeed change the Feynman rules. This is illustrated in Appendix B by adding explicit gaugino mass terms.

With the Feynman rules listed in Appendix A, we may begin to compute various properties of the scalar neutrino. Note that by using these rules, we are assuming the most simple form for the soft supersymmetry breaking terms. Given the complexity of the computation of the decay rate for $\nu_s \rightarrow \nu \tilde{\gamma}$ which

we present in Section 3, it is clear that the appropriate course of action is to always make this simplifying assumption. This, we shall argue, will provide at least a ballpark estimate and allow for further phenomenological work. Possible changes of these results due to additional soft supersymmetry breaking terms will be briefly discussed in Section 5.

3. The Decay of the Scalar Neutrino: Two-Body Decays.

The mass of the scalar neutrino is at present unconstrained by experiment. Thus, the various possible decay modes of the ν_s will vary depending on what mass assumptions are made. The first possibility is that the ν_s is the lightest supersymmetric particle. In this case, the ν_s would be stable in the model studied here.²⁵ Such a ν_s would interact with cross sections of weak-interaction size (due to the exchange of an e_s) and would therefore behave like a neutrino. The second possibility is that ω_1^+ or \tilde{z} is lighter than ν_s so that one of the following two-body decays (which can occur at the tree level) are kinematically allowed: $\nu_s \rightarrow \omega_1^+ e^-$ or $\nu_s \rightarrow \tilde{z} \nu$.²⁶ Such decays could conceivably be the most important in models which predict the existence of a wino and zino with a mass substantially less than the mass of the W and Z respectively.²⁷ To discuss this situation requires the addition of new soft supersymmetry breaking terms which can split the ω and \tilde{z} masses from those of the W and Z . This will be discussed in Section 5.

Another possible decay of the ν_s is $\nu_s \rightarrow \nu + \tilde{G}$ where \tilde{G} is the Goldstino. Technically, this decay only occurs in models where the global supersymmetry is spontaneously broken. In ref. 12, we showed that if the scale of supersymmetry breaking M_S were much larger than 1 TeV, then the decay rate (which is proportional to M_S^{-4}) would be negligible compared to other decay rates discussed in this paper. In softly broken supersymmetry, no Goldstino is required. However, if the soft supersymmetry breaking is the low energy manifestation of a spontaneously broken supergravity, then the \tilde{G} is the helicity $\pm \frac{1}{2}$ components of a massive gravitino $g_{3/2}$ and the decay $\nu_s \rightarrow \nu + g_{3/2}$ is in principle possible. However the gravitino mass is roughly $m_{g_{3/2}} \sim M_S^2/M_{\text{pl}}$ where M_{pl} is the Planck mass. In theories with $m_{g_{3/2}} \approx m_W$ ^{15,16} (which attempt to explain the

origin of the weak scale by this relation), one finds $M_S \sim 10^{11}$ GeV. Thus we may use the argument above to conclude that the decay rate into the gravitino can be ignored.

The remaining possible two-body-decay mode is $\nu_s \rightarrow \nu + \tilde{\gamma}$.²⁸ Except for the cases described above, this is expected to be the dominant decay mode. Because there is no bare $\nu_s \nu \tilde{\gamma}$ vertex in supersymmetric models, this process must occur by a one-loop graph. In our model, the contributing diagrams are given in fig. 1. Most of the graphs are divergent, but renormalizability of the theory requires that the sum of all graphs be finite. In addition, the matrix element must vanish in the supersymmetric limit. This is true because the $\nu_s \rightarrow \nu + \tilde{\gamma}$ matrix element is then related by supersymmetry to the electromagnetic form factor of the neutrino at $q^2 = 0$ which is known to vanish. This will serve as a check of our calculations.

The matrix element for $\nu_s(p) \rightarrow \tilde{\gamma}(k_1) + \nu(k_2)$ is computed to be

$$\mathcal{M} = \frac{g^2 e}{16 \sqrt{2} \pi^2} \bar{u}(k_2) \frac{1}{2} (1 + \gamma_5) v(k_1) F \quad (17)$$

where $g \equiv e/\sin \theta_W$ is the weak coupling constant, $\frac{1}{2} (1 + \gamma_5)$ is the right-handed projection operator and F is a sum of integrals obtained by evaluating the diagrams of fig. 1. The final state particles are taken to be massless. The integrals depend only on the masses M_{ν_s} , $M_{e_{sL}}$ and m_W . The dependence on m_Z and θ_W disappears from the integrals, when the relation $m_W = m_Z \cos \theta_W$ is used. Furthermore, since $M_{\tilde{\gamma}} = 0$, graph (g) in fig. 1 vanishes and hence no dependence on M_{e_R} survives. Let F_k be the integrals resulting from graph k of fig. 1. In the case of graphs (e) and (f), F_e and F_f will denote the sum over all possible graphs as indicated. Then, using the notation $r_1 \equiv M_{\nu_s}^2/m_W^2$ and $r_2 \equiv M_{e_{sL}}^2/m_W^2$, our

results are as follows:

$$F_b = 2 \left[1 + \left(\frac{1-r_1}{r_1} \right) Li_2(r_1) \right] - i\pi^{(n/2)-2} (m_W^2)^{(n/2)-2} \left(\frac{n}{n-2} \right) \Gamma \left(2 - \frac{n}{2} \right) \quad (18)$$

$$F_d = \int_0^1 \frac{dx}{1-r_2-r_1x} \log \left(x + (1-x)(r_2-r_1x) \right) \quad (19)$$

$$F_e = 2\pi^{(n/2)-2} (m_W^2)^{(n/2)-2} \Gamma \left(2 - \frac{n}{2} \right) - 3 \quad (20)$$

$$F_f = -\pi^{(n/2)-2} (m_W^2)^{(n/2)-2} \Gamma \left(2 - \frac{n}{2} \right) \quad (21)$$

$$F_g = 0 \quad (22)$$

where we have used dimensional regularization to perform the integrations in $n = 4 + \epsilon$ dimensions. The dilogarithm $Li_2(r_1)$ is discussed in Appendix C. F_a and F_c are the most complicated, although the expression simplifies when they are added resulting in:

$$\begin{aligned} F_a + F_c = & (m_W^2)^{(n/2)-2} \pi^{(n/2)-2} \Gamma \left(2 - \frac{n}{2} \right) {}_2F_1 \left(2 - \frac{n}{2}, 1; 2; 1 - r_2 \right) \\ & - r_1 \int_0^1 dx \left\{ \frac{2x}{r_2 - r_1x} \log \left(\frac{x + (1-x)(r_2 - r_1x)}{x} \right) \right. \\ & + \left(\frac{1}{1 - r_2 + r_1x} \right) \left[1 - x + \left(1 + x + \frac{1}{1 - r_2 + r_1x} \right) \right. \\ & \left. \left. \times \log(x + (1-x)(r_2 - r_1x)) \right] \right\}. \end{aligned} \quad (23)$$

It is now a simple matter to compute $F \equiv \sum_k F_k$ and show that the divergent pieces do indeed cancel (as $n \rightarrow 4$).²⁹ Thus, we may set $n = 4$ in the expression which is left. The remaining integration can be evaluated in terms of dilogarithms. The decay rate can then be calculated, and the end results is as follows:

$$\Gamma(\nu_s \rightarrow \nu + \tilde{\gamma}) = \frac{M_{\nu_s} \alpha^3}{128\pi^2 \sin^4 \theta_W} [F(r_1, r_2)]^2 \quad (24)$$

where the function F originally defined in eq. 17 is:

$$\begin{aligned}
F(r_1, r_2) = & \frac{2(1-r_1)}{r_1} Li_2(r_1) - \frac{2r_2}{r_1} \left(\frac{1}{4} \log^2 r_2 - \log^2 \left(\frac{1-r_1+r_2+\lambda}{2\sqrt{r_2}} \right) \right) \\
& + \left(\frac{2-r_1-r_2}{r_1} \right) \left(Li_2(1-r_2) - Li_2 \left(\frac{1-r_2+r_1-\lambda}{2} \right) \right) \\
& - Li_2 \left(\frac{1-r_2+r_1+\lambda}{2} \right)
\end{aligned} \tag{25}$$

and $\lambda \equiv [(1-r_1-r_2)^2 - 4r_1r_2]^{1/2}$. A discussion of the properties of the above function in Appendix C allows us to obtain the following useful limits of eq. 25.

First, if $r_1 = r_2$ then defining $r_1 = r_2 = r$ we find:

$$F(r, r) = \frac{-2(1-r)}{r} \log r \log(1-r) + \frac{2(1-2r)}{r} \left[\frac{1}{4} \log^2 r - \log^2 \left(\frac{1+\sqrt{1-4r}}{2\sqrt{r}} \right) \right]. \tag{26}$$

Second, if $r_1 = 0$, then

$$F(0, r_2) = \frac{-r_2}{1-r_2} \left(1 + \frac{r_2 \log r_2}{1-r_2} \right). \tag{27}$$

Note in particular that in the limit where $r_1, r_2 \rightarrow 0$, one finds $F(r_1, r_2) = 0$.

This verifies our claim that the matrix element for $\nu_s \rightarrow \nu + \tilde{\gamma}$ vanishes in the supersymmetric limit.

Plugging in the numbers leads to the following lifetime for the ν_s into $\nu \tilde{\gamma}$:

$$\tau = \frac{\hbar}{\Gamma} = 1.13 \times 10^{-16} \left(\frac{1}{M_{\nu_s} (GeV)} \right) \frac{1}{[F(r_1, r_2)]^2} \text{ seconds.} \tag{28}$$

A graph of $F(r_1, r_2)$ for various choices of r_1 and r_2 is shown in fig. 2. Note that $F(r_1, r_2)$ tends to be a number between 0.1 and 1.0 for interesting masses. We shall compare the lifetime given by eq. 28 with three and four body channels in the next section.

4. The Decay of the Scalar Neutrino: Three and Four-body Decays

We show in fig. 3 all possible diagrams leading to four-body final states within the model which we are using. One should note that unlike the case of $\nu_s \rightarrow \nu + \tilde{\gamma}$, many different kinds of four-body channels are accessible. To get a feeling for the expected size of the rates, let us look at the diagram which is expected to dominate, namely $\nu_s \rightarrow e^- u \bar{d} \tilde{g}$ (or $\nu_s \rightarrow e^- c \bar{s} \tilde{g}$). There are a number of enhancements worth mentioning. First, because the gluino \tilde{g} is being produced, there is a color factor of four relative to the photino for the squared amplitude. Second, the gluino couples with the strength of the strong QCD coupling (as opposed to the electromagnetic coupling of the photino $\tilde{\gamma}$). Thus, unless the scalar quarks are significantly heavier than the charged scalar leptons or the gluino mass is much larger than 5 GeV, it is clear that this process will be the dominant four-body decay mode. The neutral current processes $\nu_s \rightarrow \nu q \bar{q} \tilde{g}$ are slightly smaller in rate but are still important. We have computed the four-body decays numerically. An analytic expression may be obtained for the dominant rate by using the method discussed in Appendix D. In the limit that $M_{\nu_s} \ll M_{u,L}, m_W$ (and all final state particles are taken as massless), the result is:

$$\Gamma(\nu_s \rightarrow e^- u \bar{d} \tilde{g}) = \frac{\alpha^2 \alpha_s}{11520 \pi^2 \sin^4 \theta_W} \frac{M_{\nu_s}^9}{m_W^4 M_{u,L}^4}. \quad (29)$$

We may compare this with eq. 28. For example, if $M_{u,L} = M_{e_s} = m_W \gg M_{\nu_s}$, then:

$$\frac{\Gamma(\nu_s \rightarrow e^- u \bar{d} \tilde{g})}{\Gamma(\nu_s \rightarrow \nu \tilde{\gamma})} \approx \frac{2}{45} \left(\frac{\alpha_s}{\alpha} \right) \left(\frac{M_{\nu_s}}{m_W} \right)^8. \quad (30)$$

We see that if all the relevant supersymmetric particles have the mass of the W , then the four-body decays will be negligible. Alternatively, consider the case where $M_{u_{sL}} < M_{\nu_s}$. Then, the decay process just described is in fact the three-body decay $\nu_s \rightarrow e^- \bar{d} u_{sL}$. (Of course, the decay process is effectively a four-body one since the \bar{u}_{sL} immediately decays via $\bar{u}_{sL} \rightarrow \bar{u} + \tilde{g}$.) This decay rate is easily computed in the limit of $M_{\nu_s}, M_{u_{sL}} \ll m_W$. The result is:

$$\Gamma(\nu_s \rightarrow e^- \bar{d} u_{sL}) = \frac{G_F^2 M_{\nu_s}^5}{64\pi^3} \left[(1-x^2)(1-8x+x^2) + 12 \log x \right] \quad (31)$$

where $x \equiv M_{u_{sL}}^2/M_{\nu_s}^2$ and a color factor of 3 has been included. We may compare eq. 31 with eq. 28 evaluated when m_W^2 is large. In that limit,

$$\Gamma(\nu_s \rightarrow \nu + \tilde{\gamma}) = \frac{\alpha G_F^2 M_{\nu_s}^5 (1+x)^2}{64\pi^4} \quad (32)$$

which shows that the three-body decay will dominate as long as it is kinematically allowed (with x not too close to 1).

Finally, suppose $M_{\nu_s} < M_{u_{sL}} \approx M_{e_{sL}} \ll m_W$. From eq. 30, it is plausible that the four-body branching ratios could be significant. We have computed all the diagrams in fig. 3, explicitly, and have calculated the phase space numerically. We present our results in two cases: first, we set $M_{\nu_s} = M_{e_{sL}}$ and vary this mass (fig. 4). For convenience, all masses of scalar quarks and charged scalar leptons were set equal to $M_{e_{sL}}$. One sees that the four-body final states which include the gluino could have significant branching ratios totaling about 40% if the parameters of the supersymmetric model are in the approximate ranges discussed above. Second, we fix $M_{\nu_s} = 40$ GeV and vary M_{e_s} (which again is assumed equal to the scalar quark masses). The results are displayed in fig. 5. For $M_{e_s} < M_{\nu_s}$, we are in the regime of three-body final states (namely the

scalar quark or lepton is produced on shell). For $M_{e_s} > M_{\nu_s}$, the decay is truly a four-body decay. By putting in the explicit widths in the propagators of the scalar quarks and leptons, namely:

$$\Gamma(u_s \rightarrow \text{all}) \approx \Gamma(u_s \rightarrow u + \tilde{g}) = \frac{2}{3} \alpha_s \bar{M}_{u_s L} \quad (33a)$$

$$\Gamma(e_s \rightarrow e + \tilde{\gamma}) = \frac{1}{2} \alpha M_{e_s L} \quad (33b)$$

we can use the four-body phase space formulas in both regimes. We have checked the numerical results with the analytic expression given in eq. 31.

The conclusions one draws from fig. 5 is that the invisible mode $\nu_s \rightarrow \nu + \tilde{\gamma}$ will totally dominate (say, with branching ratio $\gtrsim 95\%$) over the various three- and four-body charged decay modes only when $M_{u_s} - M_{\nu_s} \gtrsim 15\text{-}20$ GeV. This conclusion is not particular to the choice of scalar neutrino mass; from fig. 4, one can see that such conclusions are fairly stable for a range of scalar neutrino masses below m_W . In the event that the scalar quark and scalar lepton masses are unequal, one can still use fig. 5 to estimate the various branching ratios. For example, suppose M_{u_s} is much larger than M_{ν_s} , but $M_{e_s} \approx M_{\nu_s}$. Then the branching ratio of modes containing final state gluinos are negligible. In addition, the remaining four body final states would occur with branching ratios less than 10^{-2} . Nonetheless, there are cases where rare scalar-neutrino decay modes could play an important role. For example, e^+e^- annihilation at the Z^0 resonance could be a copious source of scalar neutrinos. Hence, in such situations, certain rare decays (such as $\nu_s \rightarrow e^- \mu^+ \nu_\mu \tilde{\gamma}$) would be observable because their signature is so unusual.

Applications to the results of Section 3 and 4 have been discussed in ref. 31.

5. Complications in the Gaugino/Higgsino Sector

The computations of the previous two sections were performed using a fairly simple model, namely a supersymmetric version of the $SU(2) \times U(1)$ model of electroweak interactions with explicit mass terms for the scalar quarks and leptons which softly break the supersymmetry. However, there are other terms one could add which would softly break the supersymmetry and further complicate the model. For a theory with chiral (A, ψ, F) and gauge (V_μ, λ, D) multiplets, examples of such terms are: $Re A^3$ which is a non-supersymmetric-interaction term, $\lambda\lambda$ which is a Majorana mass term for the gaugino, and explicit mass terms for various scalar Higgs particles. In addition, low energy supergravity models often lead to an additional supersymmetric term

$$\tilde{m} \epsilon_{ij} T^i S^j \quad (34)$$

which would have to be added to the superpotential (eq. 1) and would modify a number of our results. One effect of these terms is to modify the scalar potential, eq. 3, and thereby change the ground state vacuum expectation values, eq. 4. In order to simplify the discussion, we shall mainly discuss here some of the effects resulting if we add Majorana gaugino mass terms to the model described in Section 2 (such a change by itself would leave eq. 4 unchanged).

Consider the effect of adding an explicit Majorana mass term for the gauginos. Clearly, such a term must respect $SU(2) \times U(1)$ gauge invariance. Hence the most general mass term is

$$m\lambda_a\lambda_a - m'\lambda'\lambda' + \text{h.c.} \quad (35)$$

Rewriting λ_a and λ' in terms of λ^\pm , λ_z and λ_γ , we obtain

$$m[2\lambda^+\lambda^- + \cos^2\theta_W\lambda_z\lambda_z + \sin^2\theta_W\lambda_\gamma\lambda_\gamma + 2\sin\theta_W\cos\theta_W\lambda_z\lambda_\gamma] \\ + m'[\sin^2\theta_W\lambda_z\lambda_z + \cos^2\theta_W\lambda_\gamma\lambda_\gamma - 2\sin\theta_W\cos\theta_W\lambda_z\lambda_\gamma] \quad (36)$$

We first consider the charged gaugino/higgsino sector. We may write the mass terms as³²

$$im_W(\lambda^+\psi_{T_2} + \lambda^-\psi_{S_1}) + m(\lambda^+\lambda^- + \lambda^-\lambda^+) + \text{h.c.} \quad (37)$$

When $m = 0$, the charged eigenstates ω_1 and ω_2 were half-gaugino and half-higgsino (see eq. 6) and degenerate in mass with the W^\pm . If $m \neq 0$, by diagonalizing the mass matrix, we see that the two states split in mass. The resulting states are four-component Dirac spinors and will be denoted:

$$\omega_G = \begin{pmatrix} \psi_{T_2} \cos \phi + i\lambda^- \sin \phi \\ i\bar{\lambda}^+ \sin \phi - \bar{\psi}_{S_1} \cos \phi \end{pmatrix}, \text{ mass} = m_+ \quad (38)$$

$$\omega_H = \begin{pmatrix} \psi_{S_1} \sin \phi - i\lambda^+ \cos \phi \\ i\bar{\lambda}^- \cos \phi + \bar{\psi}_{T_2} \sin \phi \end{pmatrix}, \text{ mass} = m_- \quad (39)$$

where

$$m_\pm = \sqrt{m^2 + m_W^2} \pm m \quad (40)$$

$$\cos \phi = \left(\frac{m_-}{m_+ + m_-} \right)^{1/2} \quad (41)$$

—Note that the subscripts G (and H) indicate that the fermion dominantly consists of gaugino and higgsino components respectively. In the limit of $m = 0$, $\cos \phi =$

$\sin \phi = \frac{1}{\sqrt{2}}$ and we see that ω_G and ω_H are degenerate in mass. They are related in this limit to ω_1 and ω_2 of eq. 6 as follows:

$$\omega_1 = \frac{1}{\sqrt{2}} [\omega_G + \omega_H^c] \quad (42)$$

$$\omega_2 = \frac{1}{\sqrt{2}} [\omega_H - \omega_G^c] \quad (43)$$

where the superscript C denotes charge conjugate. Note that the Feynman rules involving ω_G and ω_H must now be recomputed since the relation between interaction eigenstates and mass eigenstates has changed. These are discussed in Appendix B.

The following observations are noteworthy. First, in the model just described, one of the charged winos³³ (ω_H) is necessarily less massive than the W . This can have important consequences for phenomenology in that it might be possible to find the ω_H at current accelerators. Second, since the ω_H has dominant higgsino components, it couples less strongly to matter as compared with ω_G . However, these two remarks are extremely model dependent. For example, if the term given by eq. 34 is present and if $\tilde{m} \gg m$, then it is a wino resembling ω_G which is lightest. In fact, we can find values of m and \tilde{m} such that both winos are more massive than the W^\pm , although currently fashionable supergravity models seem to favor models with at least one light wino.

The neutral gaugino/higgsino sector is potentially more complicated. We may write the mass term as

$$im_Z \lambda_z \psi + (m \cos^2 \theta_W + m' \sin^2 \theta_W) \lambda_z \lambda_z + 2(m - m') \sin \theta_W \cos \theta_W \lambda_z \lambda_\gamma + (m' \cos^2 \theta + m \sin^2 \theta) \lambda_\gamma \lambda_\gamma + \text{h.c.} \quad (44)$$

where $\psi \equiv (\psi_{T_1} - \psi_{S_2})/\sqrt{2}$. Note that because we take $\tilde{m} = 0$ (see eq. 34), ψ_N and $(\psi_{S_2} + \psi_{T_1})/\sqrt{2}$ remain decoupled; in principle, one could have a 5×5 matrix to diagonalize. In the case described above (eq. 44), even the 3×3 matrix diagonalization does not result in a simple analytical expression. Aspects of the diagonalization in a more complicated case have been numerically worked out and are discussed in detail in refs. 34 and 35.

Here we shall make one further simplification, namely $m = m'$ in order to illustrate the results. In that case, the photino λ_γ decouples and acquires a mass $2m$. In addition, the computations of the $\lambda_Z - \psi$ sector are identical to those of the charged wino sector just discussed. The results are as follows: the spectrum of neutral fermions consists of three Majorana fermions: $\tilde{\gamma}$, \tilde{z}_H and \tilde{z}_G with masses m , μ_- and μ_+ respectively where

$$\mu_{\pm} = \sqrt{m^2 + m_Z^2} \pm m \quad (45)$$

Our notation here is that the states with tildas over them are four component Majorana spinors:

$$\tilde{\gamma} = \begin{pmatrix} i\lambda_\gamma \\ -i\bar{\lambda}_\gamma \end{pmatrix}, \tilde{z}_H = \begin{pmatrix} z_H \\ \bar{z}_H \end{pmatrix}, \tilde{z}_G = \begin{pmatrix} z_G \\ \bar{z}_G \end{pmatrix} \quad (46)$$

where

$$z_G = \psi \cos \chi - i\lambda_z \sin \chi \quad (47)$$

$$iz_H = -i\lambda_z \cos \chi - \psi \sin \chi \quad (48)$$

$$\cos \chi = \left(\frac{\mu_-}{\mu_+ + \mu_-} \right)^{1/2} \quad (49)$$

As before, the subscripts G (and H) indicate that the fermion dominantly consists of gaugino (and higgsino) components respectively. Also, new Feynman rules involving z_G and z_H are obtained in Appendix B. Note the factor of i in eq. 48; this is needed so that the neutral fermion mass eigenvalues are positive. When $m = m' = 0$, $\mu_+ = \mu_-$ and eqs. 47-49 reduce back to eqs. 12-16 of Section 2, where we identify $\tilde{z}_1 = \tilde{z}_G$ and $\tilde{z}_2 = \tilde{z}_H$.

One could now go back and recompute all the results of Section 3 with some choice of parameters m and m' . The calculations are far more complicated and we do not pursue this possibility here. However, it is worth commenting on some new subtleties which arise. Suppose one sets $m = m'$ and computes all the graphs of fig. 1. Let us concentrate on the graphs (g); these are the only graphs proportional to the number of generations of leptons and quarks. Originally in Section 3, we found $F_g = 0$. In this case, F_g is proportional to $M_{\tilde{\gamma}}^2$; however, there is a serious problem in that F_g is divergent! Clearly, this divergence cannot be cancelled by other graphs since it is proportional to the number of generations. The problem here arises because the relation $m = m'$ is not stable under radiative corrections. Working to one loop, one finds that a $\lambda_z \lambda_\gamma$ term is generated (cf. eq. 44) and therefore a new graph (fig. 6) must be added which will in the end cancel this divergence. Thus, it is clear that a calculation of $\Gamma(\nu_s \rightarrow \nu + \tilde{\gamma})$ in the presence of an explicit gaugino Majorana mass term is far more involved than the computation presented in Section 3.

Aside from being an interesting exercise in field theory calculations, we feel that there is not much more to learn by pursuing the more complicated computation. The results of Section 3 and 4 indicated that the dominant scalar-neutrino decay modes were sensitive to unknown supersymmetric masses. This conclusion

is not likely to change in more complicated softly-broken models. If anything, the results will become more dependent on unknown parameters. One interesting possibility that is worth considering briefly is the possible existence of winos and zinos lighter than the W and Z . Since some of the effects we have computed depend on the exchange of virtual winos and zinos, one might hope to enhance these effects if the winos and zinos become lighter. Unfortunately, in the present context, this does not occur. The reason for this is that the lighter particles ω_H and z_H are more higgsino-like than gaugino-like. Because the former couples to matter with strength proportional to fermion masses, their interactions are weaker than the heavier ω_G and z_G . Thus, the enhancement due to lighter masses is compensated by the weaker interactions and the overall result is not much different from the model used in Sections 3 and 4. However, it is important to keep in mind that this result is an artifact of the superpotential we have chosen. As argued earlier in this section, the conclusions can change dramatically if $\tilde{m} \gg m$ (see discussion following eq. 43). But this simply means we have been conservative in our search for supersymmetry. If supersymmetry turns out to be easier to find, then all the better!

6. Conclusions and Discussion

We have described here a simple softly broken supersymmetric model of electroweak interactions. This may be used for a phenomenological study of how supersymmetry might be revealed in current and future experimental particle physics. As an application of the model described, we considered the decay properties of the scalar neutrino. The results obtained in Sections 3 and 4 will be useful for enumerating various signatures of the scalar neutrino. The two potentially most interesting places to search for evidence of the scalar neutrino are in W and Z decay.^{31,36} In W decay, the cleanest signature requires the ν_s to decay into unobserved particles. In that case, one searches for $W \rightarrow e_s \nu_s$, $e_s \rightarrow e + \tilde{\gamma}$ and looks for an isolated electron with missing transverse momentum. In Z^0 decay, observation of the ν_s requires that the ν_s decay at least some of the time into charged particles. Then $Z^0 \rightarrow \nu_s \bar{\nu}_s$ can be best detected by observing charged hadronic jets in one hemisphere and nothing in the other hemisphere. The probability of the occurrence of such a dramatic signal can be easily computed using the results of Section 3 and 4 and is summarized in fig. 7. Details of the analysis concerning the signatures of the scalar neutrino are given in ref. 31. Observation of any one of the events just described would be a significant step in confirming the supersymmetric picture.

ACKNOWLEDGEMENTS

We are grateful to Stanley Brodsky, Michael Dine, John Ellis, Gordon Kane, Vadim Kaplunovsky, Yee Keung, Giampiero Passarino, Michael Peskin and Joe Polchinski for fruitful discussions. This work was supported in part by the Department of Energy under contract number DE-AC03-76SF00515. One of us (H.E.H.) acknowledges support by the National Science Foundation, grant PHY 8115541-02 and another of us (R.M.B.) acknowledges support by the National Science Foundation, grant PHY77-27084 (supplemented by funds from the National Aeronautics and Space Administration).

Appendix A: Feynman Rules

We list some of the relevant Feynman rules for the supersymmetric model of electroweak interactions described in Section 2 in figs. 8-13. Note that if one softly breaks the supersymmetry by adding *only* explicit mass terms for scalar leptons and quarks, then there is no change in the rules stated. (Of course, propagators and kinematics must reflect the actual masses.)

Our conventions and the Feynman rules of the standard model of electroweak interactions can be found in ref. 37. We always represent 0, $\frac{1}{2}$, and 1 particles by dashed, solid and wavy lines respectively. Dealing with Majorana fermions can sometimes be confusing. We have found the rules given in the appendix of ref. 38 to be useful since it makes it possible to use the familiar four-component language for fermions.

The following comments may be helpful. In fig. 8, for example, the direction of the arrows on the final state line gives the flow of electric charge. The momenta are also defined as indicated by the arrows but the outgoing lines are labelled by the names of the emitted particles. So, in fig. 8(b), $Z^0 \rightarrow e^+e^-$ whereas the arrow indicates the flow of negative charge.

In fig. 11, we give the rules in terms of \tilde{z}_1 and \tilde{z}_2 as defined in eq. 16. The rules for the \tilde{z}_2 vertices are obtained from the corresponding \tilde{z}_1 vertices by multiplication by $-i$ as illustrated in fig. 11(d). This factor i is a consequence of the factor i which appears on the left hand side of eq. 11. Alternatively, one could write these rules in terms of \tilde{z} and \tilde{z}^c (see eq. 7). However, this is only

possible in the special case where the zino masses are degenerate. One finds an interaction:

$$\begin{aligned} & \frac{ig}{2\sqrt{2}\cos\theta_W} [\bar{\nu}(1+\gamma_5)\tilde{z}\nu_s + (\sin^2\theta_W - \cos^2\theta_W)\bar{e}(1+\gamma_5)\tilde{z}e_{sL}] \\ & - \frac{i\sqrt{2}g\sin^2\theta_W}{2\cos\theta_W}\tilde{z}^c(1+\gamma_5)e e_{sR} + \text{h.c.} \end{aligned} \quad (\text{A.1})$$

This form is often more convenient when only left-handed fermions appear. Note that $\psi^c = C\bar{\psi}^T$ where $C = i\gamma^2\gamma^0$ in the standard basis.

Finally, note that we have only written out explicitly rules involving leptons. One can obtain rules involving quarks in a straightforward manner. As an example, consider the rules given by fig. 11(a)-(c). They can be summarized by one rule:

$$\frac{ig(1+\gamma_5)}{2\cos\theta} (T_3 - Q\sin^2\theta_W) \quad (\text{A.2})$$

where $T_3 = \frac{1}{2} - \frac{1}{2}$, and 0 and $Q = 0, -1$, and $+1$ for $\nu, e^-,$ and e^+ respectively. Thus, formula (A.2) can now be used for zino interaction with quark-scalar quark pairs. Similar considerations can be applied elsewhere.

We have also omitted writing out explicit rules involving the gluino. The vertices for $qq_s\tilde{g}$ are easily obtained from fig. 10(a)-(b) by replacing e with the strong coupling constant g_s . Color factors are computed in the usual fashion.

Appendix B: The Effect of Gaugino Majorana Masses

When explicit Majorana mass terms for the gauginos are added, the relation between “interaction” eigenstates and “mass” eigenstates is changed. The Lagrangian, expressed in terms of interaction eigenstates, is unchanged except for the additional new term. But, the Feynman rules are expressed in terms of mass eigenstates and hence they are modified. We list here some of the relevant new interactions.

1. $\omega - e_s - \nu$ and $\omega - e - \nu_s$:

$$\frac{ig}{2} \left[\bar{e}(1 + \gamma_5)(\omega_G \sin \phi + \omega_H^c \cos \phi)\nu_s + \text{h.c.} \right. \\ \left. + \bar{\nu}(1 + \gamma_5)(\omega_H \cos \phi - \omega_G^c \sin \phi)e_{sL} + \text{h.c.} \right] \quad (B.1)$$

(See eqs. 38-41 for definitions of the angle ϕ , and states ω_G, ω_H .) One curious feature of eq. B.1 is the appearance of both ω_G and ω_G^c (and likewise ω_H and ω_H^c). One consequence is the appearance of fermion-number violating propagators since, for example, the process $\bar{\nu} e_{sL}^- \rightarrow \omega_G^- \rightarrow e^- \nu_s$ is allowed by eq. B.1. The way to deal with such processes is by using the same fermion-number violating propagators which were used in the appendix of ref. 40 for fermion-number violating propagators of Majorana fermions. Note that it is easy to check that in the limit of $m \rightarrow 0$, the linear combinations given by eqs. 42 and 43 are the appropriate ones which appear in the rules of fig. 12(c),(d). Namely, $e^- \nu_s$ decouples from ω_2 and $e_s \nu$ decouples from ω_1 in this limit.

2. $W - \omega - \tilde{\gamma}$:

$$-\frac{ie}{2} W_\mu^+ \tilde{\gamma} \gamma_\mu (1 + \gamma_5)(\omega_G \sin \phi + \omega_H^c \cos \phi) + \text{h.c.} \\ -\frac{ie}{2} W_\mu^- \tilde{\gamma} \gamma_\mu (1 + \gamma_5)(\omega_G^c \sin \phi - \omega_H \cos \phi) + \text{h.c.} \quad (B.2)$$

3. $\bar{z} - \nu - \nu_3$ and $\bar{z} - e - e_3$:

We use the notation given by eqs. 47-49, which is relevant to the special case of $m = m'$. the resulting interaction is

$$\begin{aligned} & \frac{ig}{2\sqrt{2}\cos\theta_W} \left\{ \bar{\nu}(1+\gamma_5)(\bar{z}_G \sin\chi - i\bar{z}_H \cos\chi)\nu_3 \right. \\ & \quad + (\sin^2\theta_W - \cos^2\theta_W)\bar{e}(1+\gamma_5)(\bar{z}_G \sin\chi - i\bar{z}_H \cos\chi)e_{sL} \\ & \quad \left. - 2\sin^2\theta_W(\bar{z}_G \sin\chi - i\bar{z}_H \cos\chi)(1+\gamma_5)e e_{sR} \right\} \\ & \quad + \text{h.c.} \end{aligned} \tag{B.3}$$

An expression like this is (in principle) easily generalized to the case of $m \neq m'$.

Appendix C: Mathematical Properties of $F(r_1, r_2)$

The function $F(r_1, r_2)$ defined in eq. 17 (where $r_1 \equiv M_{\nu_S}^2/m_W^2$ and $r_2 \equiv M_{\nu_{S_L}}^2/m_W^2$) is proportional to the effective interaction matrix element for $\nu_s \nu \tilde{\gamma}$. At one loop, it was calculated in Section 2 and the final expression is given by eq. 25. In this appendix, we shall study the mathematical properties of this function.

It is useful to define a secondary function

$$G(r_1, r_2) = \frac{1}{r_1} \left[Li_2(1-r_2) - Li_2\left(\frac{1-r_2+r_1-\lambda}{2}\right) - Li_2\left(\frac{1-r_2+r_1+\lambda}{2}\right) \right] \quad (C.1)$$

where $\lambda \equiv [(1-r_1-r_2)^2 - 4r_1r_2]^{1/2}$. The dilogarithm is defined as³⁹

$$Li_2(x) = - \int_0^x \frac{\log(1-t)}{t} dt \quad (C.2)$$

It is an analytic function defined in the complex plane cut from $x = 1$ to $x = \infty$. For real $x \leq 1$, $Li_2(x)$ is manifestly real. A useful integral expression for $G(r_1, r_2)$ is:

$$G(r_1, r_2) = \frac{1}{r_1} \int_0^1 \frac{dx}{x} \log \left(1 - \frac{r_1 x(1-x)}{1-x+r_2 x} \right) \quad (C.3)$$

For $0 \leq r_1 \leq (1+r_2-2\sqrt{r_2})$, the arguments of the dilogarithms in eq. C.1 are real. For $(1+r_2-2\sqrt{r_2}) \leq r_1 \leq (1+r_2+2\sqrt{r_2})$, λ is purely imaginary so that $G(r_1, r_2)$ is still real. In this range of parameters, the following expression in place of (C.1) is more useful:

$$G(r_1, r_2) = \frac{1}{r_1} [Li_2(1-r_2) - 2Li_2(\sqrt{r_1}, \theta)] \quad (C.4)$$

where $\cos \theta \equiv (1+r_1-r_2)/(2\sqrt{r_1})$, $0 \leq \theta \leq \pi$ and

$$Li_2(x, \theta) = - \frac{1}{2} \int_0^x \frac{\log(t^2 - 2t \cos \theta + 1) dt}{t} \quad (C.5)$$

or equivalently, $Li_2(x, \theta) = Re Li_2(x e^{i\theta})$ for x real.

The properties of the functions $Li_2(x)$ and $Li_2(x, \theta)$ allow us to deduce the following interesting special cases:

$$G(0, r_2) = \frac{-1}{1-r_2} \left[1 + \frac{r_2 \log r_2}{1-r_2} \right] \quad (C.6)$$

$$G(r_1, 0) = -\frac{1}{r_1} Li_2(r_1) \quad (C.7)$$

$$G(r_1, 1) = -\frac{2}{r_1} \left[\sin^{-1} \left(\frac{\sqrt{r_1}}{2} \right) \right]^2 \quad (C.8)$$

where $-\frac{\pi}{2} \leq \sin^{-1} \left(\frac{\sqrt{r_1}}{2} \right) \leq \frac{\pi}{2}$ in eq. C.8.

For $r_1 \geq (1 + r_2 + 2\sqrt{r_2})$, $G(r_1, r_2)$ is a complex-valued function. Its value can be deduced by analytic continuation of eq. C.1; however extreme care must be taken with defining the dilogarithms above and below the cut.

With the properties of $G(r_1, r_2)$ already described, it is straightforward to obtain the properties of $F(r_1, r_2)$ defined by eq. 25. We rewrite this function below:

$$F(r_1, r_2) = \frac{2(1-r_1)}{r_1} Li_2(r_1) + (2-r_1-r_2)G(r_1, r_2) - \frac{2r_2}{r_1} \left(\frac{1}{4} \log^2 r_2 - \log^2 \left(\frac{1-r_1+r_2+\lambda}{2\sqrt{r_2}} \right) \right) \quad (C.9)$$

The only remaining subtlety involves the logarithm when λ is purely imaginary.

In that case, we use:

$$\log^2 \left(\frac{1-r_1+r_2+\lambda}{2\sqrt{r_2}} \right) = - \left(\cos^{-1} \left(\frac{1-r_1+r_2}{2\sqrt{r_2}} \right) \right)^2 \quad (C.10)$$

which is used when $1 + r_2 - 2\sqrt{r_2} \leq r_1 \leq 1 - r_2 + 2\sqrt{r_2}$. The arccosine then takes on values between 0 and π .

Equations (26) and (27) are now easily derived. Other limits of interest are:

$$\begin{aligned}
 F(r_1, 0) &= -Li_2(r_1) \\
 \lim_{r_2 \rightarrow \infty} F(r_1, r_2) &= -\log^2 r_2
 \end{aligned}
 \tag{C.11}$$

These limits are helpful to check the curves given in fig. 2.

One final observation: $r_1 \geq (1-r_2+2\sqrt{r_2})$ corresponds to $M_{\nu_e} \geq M_{e_e} + m_W$ which means that a physical threshold has been crossed. Hence, $F(r_1, r_2)$ becomes complex there as it should. Note that the complexity of $F(r_1, r_2)$ occurs, because cutting the triangle graph results in real processes on both sides of the cut. For example, if $M_{e_e} < M_{\nu_e} < m_W$, then real three body decays can occur but this does not alter the reality of $F(r_1, r_2)$.

Appendix D: Computation of Four-body Decay Rates

We provide here some of the necessary details for the analytic calculation of the four body decay rate of the scalar neutrino. We have found very useful the appendix of ref. 40 which provides a nice technique for computing massless four-body phase space.

The formula for the decay rate of the ν_s with a four-momentum p into particles of four-momenta k_i is:

$$\Gamma = \frac{(2\pi)^{-8}}{2M_{\nu_s}} \int \prod_{i=1}^4 \frac{d^3k_i}{2E_i} \delta^4(p - k_1 - k_2 - k_3 - k_4) |\tilde{\mathcal{M}}|^2 \quad (D.1)$$

where $|\tilde{\mathcal{M}}|^2$ is the squared matrix element averaged over initial states and summed over final states (with all group-theoretical factors included). Consider now the process $\nu_s(p) \rightarrow e^-(k_3) + u(k_1) + \bar{d}(k_2) + \bar{g}(k_4)$ (see fig. 3(e)) with four-momenta as indicated, where all final particle masses are neglected. Then $|\tilde{\mathcal{M}}|^2$ is given by:

$$\begin{aligned} |\tilde{\mathcal{M}}|^2 = & \frac{64(4\pi)^3 \alpha^2 \alpha_s (k_1 \cdot k_4)}{\sin^4 \theta_W [M_W^2 - (k_1 + k_2 + k_4)^2]^2 [M_{u_s}^2 - (k_1 + k_4)^2]^2} \\ & \times [(k_1 \cdot k_2)(k_1 \cdot k_3) + (k_1 \cdot k_2)(k_3 \cdot k_4) + (k_1 \cdot k_3)(k_2 \cdot k_4) \\ & + (k_1 \cdot k_4)(k_3 \cdot k_4) - (k_2 \cdot k_3)(k_1 \cdot k_4)] \end{aligned} \quad (D.2)$$

Note that we have included the color factor: $\text{Tr } T^a T^a = 4$. For simplicity, we will evaluate eq. D.1 in the limit that $M_{\nu_s} \ll m_W, M_{u_s}$, which allow us to replace the propagator factors in eq. D.2 with $(m_W M_{u_s})^{-4}$. To carry out the integration, let $N = p - k_1 - k_4$. Then we first compute:

$$\begin{aligned} \int \frac{d^3k_2}{2E_2} \frac{k^3 k_3}{2E_3} \delta^4(N - k_2 - k_3) [(k_1 \cdot k_2)(k_1 \cdot k_3) + (k_1 \cdot k_2)(k_3 \cdot k_4) \\ + (k_1 \cdot k_3)(k_2 \cdot k_4) + (k_2 \cdot k_4)(k_3 \cdot k_4) - (k_2 \cdot k_3)(k_1 \cdot k_4)] \end{aligned} \quad (D.3)$$

This is easily evaluated using

$$\int \frac{d^3k_2}{2E_2} \frac{d^3k_3}{2E_3} k_2 \cdot r k_3 \cdot s \delta^4(N - k_2 - k_3) \quad (D.4)$$

$$= \frac{\pi}{24} [2(q \cdot N)(s \cdot N) + (q \cdot s)N^2]$$

and

$$\int \frac{d^3k_2}{2E_2} \frac{d^3k_3}{2E_3} k_2 \cdot k_3 \delta^4(N - k_2 - k_3) = \frac{\pi N^2}{4} \quad (D.5)$$

Thus, for $M_{\nu_s} \ll m_W, M_{u_s}$, we find:

$$\Gamma = \frac{2\alpha^2\alpha_s}{3\pi^4 M_{\nu_s} M_W^4 M_{u_s}^4} \int \frac{d^3k_1}{2E_1} \frac{d^3k_4}{2E_4} k_1 \cdot k_4 [(N \cdot (k_1 + k_4))^2 - 2N^2 k_1 \cdot k_4] \quad (D.6)$$

where $N = p - k_1 - k_4$. To evaluate the remaining integrals, choose the rest frame $\vec{p} = 0$, let \vec{k}_4 be along the z -axis and let \vec{k}_1 lie in the $x - z$ plane. Define $\cos \theta = \hat{k}_1 \cdot \hat{k}_4$. In this frame, using massless kinematics and denoting the respective energies by $E_3 = |\vec{k}_3|$ and $E_4 = |\vec{k}_4|$, we find:

$$\Gamma = \frac{4\alpha^2\alpha_s M_{\nu_s}}{3\pi^2 m_W^4 M_{u_s}^4} \int E_1 dE_1 E_4 dE_4 dx E_1 E_4 (1-x) [(E_1 + E_4)^2 - 2E_1 E_4 (1-x)] \quad (D.7)$$

where $x \equiv \cos \theta$. The limits of integration can be obtained from ref. 40:

$$(i) \quad 0 \leq E_4 \leq \frac{1}{2} M_{\nu_s}$$

$$(ii) \quad 0 \leq E_1 \leq \frac{1}{2} M_{\nu_s}$$

$$(iii) \quad \text{If } 0 \leq E_1 \leq \frac{1}{2} M_{\nu_s} - E_4, \text{ then } -1 \leq x \leq 1$$

$$(iv) \quad \text{If } \frac{1}{2} M_{\nu_s} - E_4 \leq E_1 \leq \frac{1}{2} M_{\nu_s}, \text{ then}$$

$$-1 \leq x \leq 1 - \left(\frac{2M_{\nu_s}(E_1 + E_4) - M_{\nu_s}^2}{2E_1 E_4} \right)$$

The integration now is straightforward, though tedious. The results of the integral is $M_{\nu}^8/((15)(2^{10}))$. Inserting this into eq. D.7, we end up with the result given by eq. 29 in the text.

We used the analytic calculation above as a check of our numerical integration.

REFERENCES

1. M.A.B. Beg and A. Sirlin, *Phys. Rep.* **88**, 1 (1982).
2. P. Langacker, *Phys. Rep.* **72**, 185 (1981).
3. H. Georgi, H. R. Quinn and S. Weinberg, *Phys. Rev. Lett.* **33**, 451 (1974); E. Gildener, *Phys. Rev.* **D14**, 1667 (1976); A. J. Buras, J. Ellis, M. K. Gaillard, and D. V. Nanopoulos, *Nucl. Phys.* **B135**, 66 (1978); C. Sachrajda, *Phys. Lett.* **98B**, 74 (1981); C. H. Llewellyn Smith and G. G. Ross, *Phys. Lett.* **105B**, 38 (1981); Y. Kazama and Y.-P. Yao, *Phys. Rev.* **D25**, 1650 (1982).
4. H. Georgi and A. Pais, *Phys. Rev.* **D10**, 539 (1974); S. Weinberg, *Phys. Rev.* **D13**, 974 (1976); L. Susskind, *Phys. Rev.* **D20**, 2619 (1979); G. 't Hooft in "Recent Developments in Gauge Theories", proceedings of the NATO Advanced Study Institute, Cargese, 1979, edited by G. 't Hooft, *et al.* (Plenum, New York, 1980); M. Veltman, *Acta Phys. Pol.* **B12**, 437 (1981).
5. E. Witten, *Nucl. Phys.* **B185**, 513 (1981).
6. I. Hinchliffe and L. Littenberg in Proceedings of the 1982 DPF Summer Study of Elementary Particle Physics and Future Facilities, p. 242 (American Physical Society, New York, 1982); D. V. Nanopoulos, A. Savoy-Navarro, and Ch. Tao, Proceedings of the Supersymmetry versus Experiment Workshop, Ref. Th.3311/EP.82/63-CERN (1982) to be published in *Physics Reports*.
7. For a review of theoretical and phenomenological work regarding the search for supersymmetry in future experiments, see a review article by H. E. Haber and G. L. Kane, to be published in *Physics Reports*.

8. The L and R subscripts indicate that these particles are partners to the left- and right-handed parts of the fermion f . Whether f_{sL} and f_{sR} are the physical mass eigenstates rather than some other linear combination is model-dependent. Phenomenologically, the absence of parity violations in the strong interactions can impose significant constraints (e. g. $M_{f_{sL}} \approx M_{f_{sR}}$ for the scalar partners of the u and d quarks if the masses are not too heavy) as shown in ref. 9.
9. M. Suzuki, Phys. Lett. **115B**, 40 (1982); M. J. Duncan, Nucl. Phys. **B214**, 21 (1983).
10. Recent limits on masses of supersymmetric particle were summarized by S. Yamada at the 1983 International Symposium on Lepton and Photon Interactions at High Energies. Previous published limits are: H. J. Behrend *et al.*, Phys. Lett. **114B**, 287 (1982); W. Bartel *et al.*, Phys. Lett. **114B**, 211 (1982); R. Brandelik *et al.*, Phys. Lett. **117B**, 365 (1982); D. P. Barber *et al.*, Phys. Rev. Lett. **45**, 1904 (1980); W. T. Ford *et al.*, SLAC-PUB-2986 (1982); Y. Ducros, Acta Phys. Pol. **B14**, 589 (1983); L. Gladney, *et al.*, SLAC-PUB-3178 (1983); E. Fernandez, *et al.*, SLAC-PUB-3231 (1983).
11. G. L. Kane and W. B. Rolnick, preprint UMTH 83-14 (1983).
12. R. M. Barnett, K. S. Lackner and H. E. Haber, Phys. Lett. **126B**, 64 (1983).
13. P. Fayet, Phys. Lett. **69B**, 489 (1977); **84B**, 416 (1979); S. Weinberg, Phys. Rev. **D25**, 287 (1982); M. Dine and W. Fischler, Phys. Lett. **110B**, 227 (1982); L. J. Hall and I. Hinchliffe, Phys. Lett. **112B**, 351 (1982); C. R. Nappi and B. A. Ovrut, Phys. Lett. **113B**, 175 (1982); L. Alvarez-Gaume, M. Claudson and M. B. Wise, Nucl. Phys. **B207**, 96 (1982).

14. E. Cremmer, S. Ferrara, L. Girardello and A. van Proeyer, Phys. Lett. 116B, 231 (1982); Nucl. Phys. B212, 413 (1983); L. Hall, J. Lykken and S. Weinberg, Phys. Rev. D27, 2359 (1983).
15. A. H. Chamseddine, R. Arnowitt and P. Nath, Phys. Rev. Lett. 49, 970 (1982); Phys. Lett. 120B, 145 (1983); Phys. Lett. 121B, 33 (1983); R. Barbieri, S. Ferrara and C. A. Savoy, Phys. Lett. 119B, 343 (1982); E. Cremmer, P. Fayet and L. Girardello, Phys. Lett. 120B, 41 (1983).
16. H. P. Nilles, Phys. Lett. 115B, 193 (1982); Nucl. Phys. B217, 366 (1983); L. Ibanez, Phys. Lett. 118B, 73 (1982); Nucl. Phys. B218, 514 (1983); L. Alvarez-Gaume, J. Polchinski and M. B. Wise, Nucl. Phys. B221, 495 (1983); J. Ellis, J. S. Hagelin, D. V. Nanopoulos and K. Tamvakis, Phys. Lett. 125B, 275 (1983); M. Claudson, L. J. Hall and I. Hinchliffe, preprint LBL-15948 (1983); C. Kounnas *et al.*, CERN preprints Ref. TH.3651, 3657 (1983).
17. L. Girardello and M. T. Grisaru, Nucl. Phys. B194, 65 (1982).
18. P. Fayet, Nucl. Phys. B90, 104 (1975).
19. Fayet's model (ref. 18) was subsequently studied in detail in R. K. Kaul, Phys. Lett. 109B, 19 (1982); R. K. Kaul and P. Majumdar, Nucl. Phys. B199, 36 (1982).
20. Such models have been recently studied in the context of supergravity. See ref. 15.
21. This possibility may not be entirely ruled out. For a discussion of spontaneous breaking of lepton number in the context of supersymmetry, see L. J. Hall and M. Suzuki, preprint LBL-16150 (1983).
22. We will often use two-component notation for fermions and later trans-

late our results to four-component notation. For a recent description of these notations and an introduction to supersymmetry in general, see J. Wess and J. Bagger, *Supersymmetry and Supergravity* (Princeton University Press, Princeton, New Jersey, 1983).

23. For the standard procedures for constructing supersymmetric Lagrangians, see P. Fayet and S. Ferrara, *Phys. Rep.* 32C, 244 (1977); J. Wess and J. Bagger, ref. 22.
24. The fact that both $\langle A_S \rangle$ and $\langle A_T \rangle$ are equal is a feature of the superpotential chosen in eq. 1. Models which do not contain an $SU(2) \times U(1)$ singlet superfield N can be arranged such that $\langle A_S \rangle$ and $\langle A_T \rangle$ are independent. See, for example, ref. 16.
25. The stability of the lightest supersymmetry particle occurs here because of an unbroken discrete R -parity which is $+1$ for "ordinary" particles and -1 for their supersymmetric particles. Models exist where R -parity is broken but such models often lead to baryon or lepton number violation. See ref. 21.
26. The decay $\nu_S \rightarrow W^+ e_{SL}^-$ is not too interesting since it would require a very massive ν_S which could not be produced by experiments in the near future.
27. S. Weinberg, *Phys. Rev. Lett.* 50, 387 (1983); R. Arnowitt, A. H. Chamseddine, and P. Nath, *Phys. Rev. Lett.* 50, 232 (1983); P. Fayet, *Phys. Lett.* 125B, 178 (1983); B. Grinstein, J. Polchinski, and M. B. Wise, Caltech preprint CALT-68-1038 (1983).
28. Here again, we assume the simplest version of our model in which case the supersymmetric partner of the photon (the photino $\tilde{\gamma}$) is the appro-

appropriate mass eigenstate. More complicated possibilities will be discussed in Section 5.

29. The following identity for the hypergeometric function can be derived:

$$\lim_{n \rightarrow 4} \Gamma\left(2 - \frac{n}{2}\right) {}_2F_1\left(2 - \frac{n}{2}, 1; 2; z\right) = \Gamma\left(2 - \frac{n}{2}\right) + 1 + \frac{1-z}{z} \log(1-z).$$

For useful formulas, see ref. 30.

30. A. Erdélyi, *et al.*, *Higher Transcendental Functions, Vol. I*, (McGraw-Hill, New York, 1953).
31. R. M. Barnett, H. E. Haber and K. S. Lackner, *Phys. Rev. Lett.* **51**, 176 (1983); SLAC-PUB-3225 (1983).
32. Note that barring a supersymmetric term $\tilde{m} \epsilon_{ij} T^i S^j$ appearing in the superpotential, there will be no $\psi_{T_2} \psi_{S_1}$ mass term appearing. If such a term does appear (as it probably will in more realistic models, see e.g. ref. 16), then these considerations are relevant if $\tilde{m} \ll m$.
33. The term “wino” is probably inappropriate here but we shall continue to use it to generically refer to ω_G and ω_H .
34. J.-M. Frere and G. L. Kane, *Nucl. Phys.* **B223**, 331 (1983).
35. J. Ellis and G. G. Ross, *Phys. Lett.* **117B**, 397 (1983); J. Ellis, J. Hagelin, D. V. Nanopoulos and M. Srednicki, *Phys. Lett.* **127B**, 233 (1983); J. Ellis, *et al.*, SLAC-PUB-3152 (1983).
36. R. Barbieri, N. Cabibbo, L. Maiani and S. Petrarca, *Phys. Lett.* **127B**, 458 (1983); D. A. Dicus, S. Nandi, W. W. Repko and X. Tata, *Phys. Rev. Lett.* **51**, 1030 (1983).
37. I.J.R. Aitchison and A.J.G. Hey, *Gauge Theories in Particle Physics* (Adam Hilger LTD, Bristol, 1982).

38. S. K. Jones and C. H. Llewellyn Smith, Nucl. Phys. B217, 145 (1983).
39. L. Lewin, *Polylogarithms and Associated Functions* (Elsevier North-Holland, New York, 1981).
40. Y. Singh, Phys. Rev. 161, 1497 (1967).

Table 1

Superfield content of a supersymmetric $SU(2) \times U(1)$ model. We list the gauge and chiral multiplets of our model. The charge Q is obtained via $Q = T_3 + Y/2$. The label r refers to multiple generations of quarks, leptons and their scalar partners.

Superfield	Label	Description	Particle Content
<u>Gauge Multiplets :</u>			
V^a	$a = 1, 2, 3$	$SU(2)_W$ gauge multiplet	(V_μ^a, λ^a)
V'		$U(1)_{Y'}$ gauge multiplet	(V'_μ, λ')
<u>Chiral Multiplets :</u>			
L_r^j	$j = 1, 2$	$Y = -1, SU(2)_W$ doublet	$\{(\nu_s, e_{sL}^-); (\nu, e^-)_L\}$
R_r		$Y = 2, SU(2)_W$ singlet	$\{e_{sR}^+, e_R^+\}$
Q_r^j	$j = 1, 2$	$Y = 1/3, SU(2)_W$ doublet	$\{(u_{sL}, d_{sL}); (u, d)_L\}$
U_r		$Y = -4/3, SU(2)_W$ singlet	$\{\bar{u}_{sR}, \bar{u}_R\}$
D_r		$Y = 2/3, SU(2)_W$ singlet	$\{\bar{d}_{sR}, \bar{d}_R\}$
S^j	$j = 1, 2$	$Y = 1, SU(2)_W$ doublet	$\{(A_{S1}, A_{S2}); (\psi_{S1}, \psi_{S2})\}$
T^j	$j = 1, 2$	$Y = -1, SU(2)_W$ doublet	$\{(A_{T1}, A_{T2}); (\psi_{T1}, \psi_{T2})\}$
N		$Y = 0, SU(2)_W$ singlet	$\{A_N, \psi_N\}$

FIGURE CAPTIONS

1. One loop diagrams for $\nu_s \rightarrow \nu \tilde{\gamma}$. These are the contributing graphs in a supersymmetric $SU(2) \times U(1)$ model with the supersymmetry broken only by explicit mass terms for the scalar quarks and leptons. Note that in (e), the loop consists of either $W^- \omega_2^+$ or $W^+ \omega_1^-$. Similarly in (f) with H replacing W . In (g) the loop consists of either $e_{sL}^- e^+$ or $e_{sR}^+ e^-$ as well as all relevant members from other generations of leptons, quarks and their scalar partners.
2. A graph of the function $F(r_1, r_2)$ defined by eq. 25 for various values of r_1 and $r_2 = ar_1$. The function is actually negative definite, so we plot its absolute value.
3. Four-body decays of the scalar neutrino. See caption to fig. 1. Note that we use the symbol u and d for all up-type and down-type quarks, etc. For convenience, the Cabibbo angle is neglected.
4. Branching ratio for four-body models of the scalar neutrino. We label the various modes as follows:

(a) $e^- u \bar{d} \tilde{g} + e^- c \bar{s} \tilde{g}$;

(b) $\sum_i \nu \bar{q}_i q_i \tilde{g}$;

(c) $e^- u \bar{d} \tilde{\gamma} + e^- c \bar{s} \tilde{\gamma}$;

(d) $\nu e^+ e^- \tilde{\gamma}$;

(e) $\nu \mu^+ \mu^- \tilde{\gamma}$ or $\nu \tau^+ \tau^- \tilde{\gamma}$;

The rates for $\nu \mu^+ e^- \tilde{\gamma}$, and $\nu \tau^+ e^- \tilde{\gamma}$ and $\sum_i \nu \bar{q}_i q_i \tilde{\gamma}$ occur approximately at the level of (d). We use a value of $\alpha_s = 0.2$. We have taken the charged scalar lepton and scalar quark masses to be equal.

5. Branching ratio of charged modes as a function of M_{e_s} (which is assumed to be equal to M_{u_s}). We have chosen $M_{\nu_s} = 40$ GeV. Note that for $M_{e_s} < M_{\nu_s}$, the dominant decays are actually three-body decays containing a physical e_s (or u_s) in the final state. The labelling here is the same as in Fig. 4 except that we have to distinguish between d (which corresponds to $\nu_\ell \ell^+ e^- \tilde{\gamma}$ final states) and d' (which corresponds to $\nu \bar{q} q \tilde{\gamma}$).
6. Contributing graph to $\nu_s \rightarrow \nu \tilde{\gamma}$ if $m_{\tilde{\gamma}} \neq 0$. In general, $\tilde{\gamma}$ mixes with \tilde{z}_1, \tilde{z}_2 and a counterterm is required. When added to the graphs in fig. 1, the resulting decay rate would be finite. If $m_{\tilde{\gamma}} = 0$, this counterterm is not necessary.
7. Fraction of $e^+ e^- \rightarrow \nu_s \nu_s$ events where one of the scalar neutrinos decays into charged particles and the other one decays into invisible neutrals (solid line); and fraction of events where both scalar neutrinos decay into charged particles (dashed lines). We have chosen $M_{\nu_s} = 20$ GeV; the graph follows from the results of Sections 3 and 4.
8. Feynman rules for the coupling of neutral gauge bosons to fermion and scalar pairs.
9. Feynman rules for the coupling of charged gauge bosons into pairs of ordinary and supersymmetric fermions and bosons. The photino is massless, the \tilde{z} is degenerate in mass with the Z^0 and the ω_1^- and ω_2^+ are degenerate in mass with the W^+ .
10. Feynman rules for the coupling of photinos and winos to a lepton-scalar lepton pair. (See the caption to fig. 9.)
11. Feynman rules for the coupling of zinos to a lepton-scalar lepton pair.

We have omitted two diagrams involving \tilde{z}_2 analogous to (b) and (c). These rules are obtained in the same way as getting (d) from (a), i.e. by multiplying by $-i$. The zinos \tilde{z}_1 and \tilde{z}_2 are Majorana fermions which are degenerate in mass with the Z^0 . (See the caption to fig. 9.)

12. Feynman rules for the coupling of the charged Higgs bosons. The H^\pm and W^\pm are degenerate in mass (see the caption to fig. 9).
13. Feynman rules for the coupling of one of the neutral Higgs bosons. The H^0 is degenerate in mass with the Z^0 (see the caption to fig. 9).

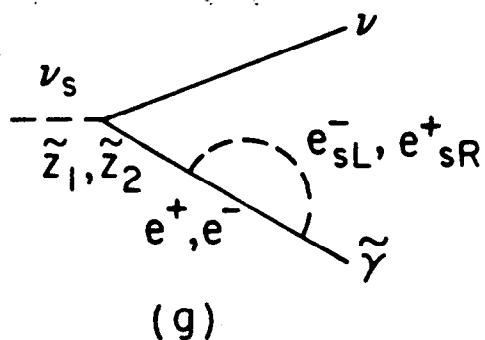
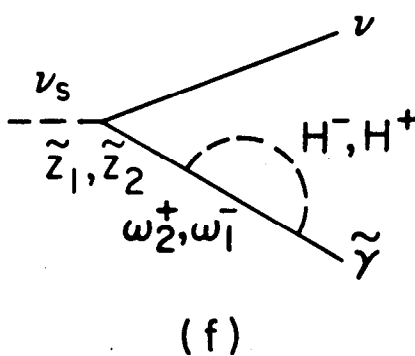
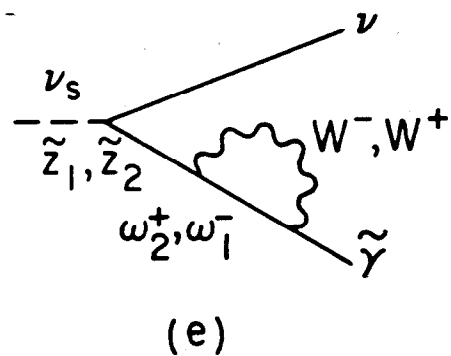
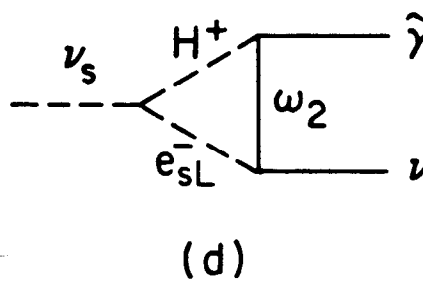
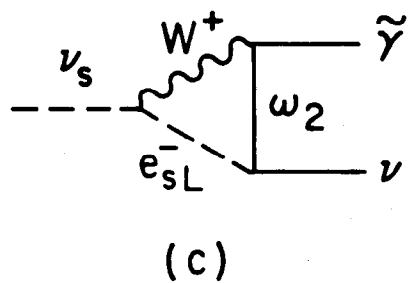
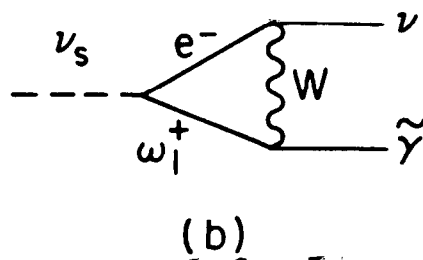
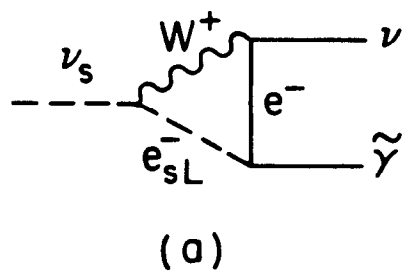
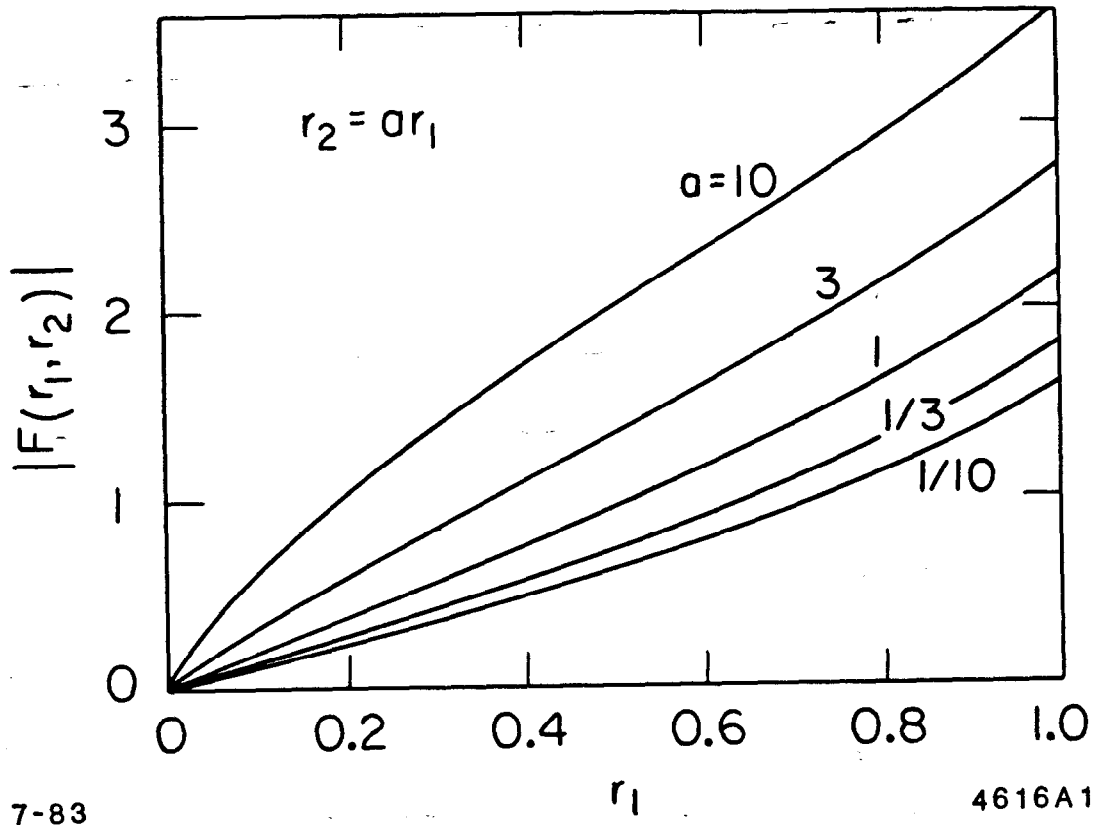


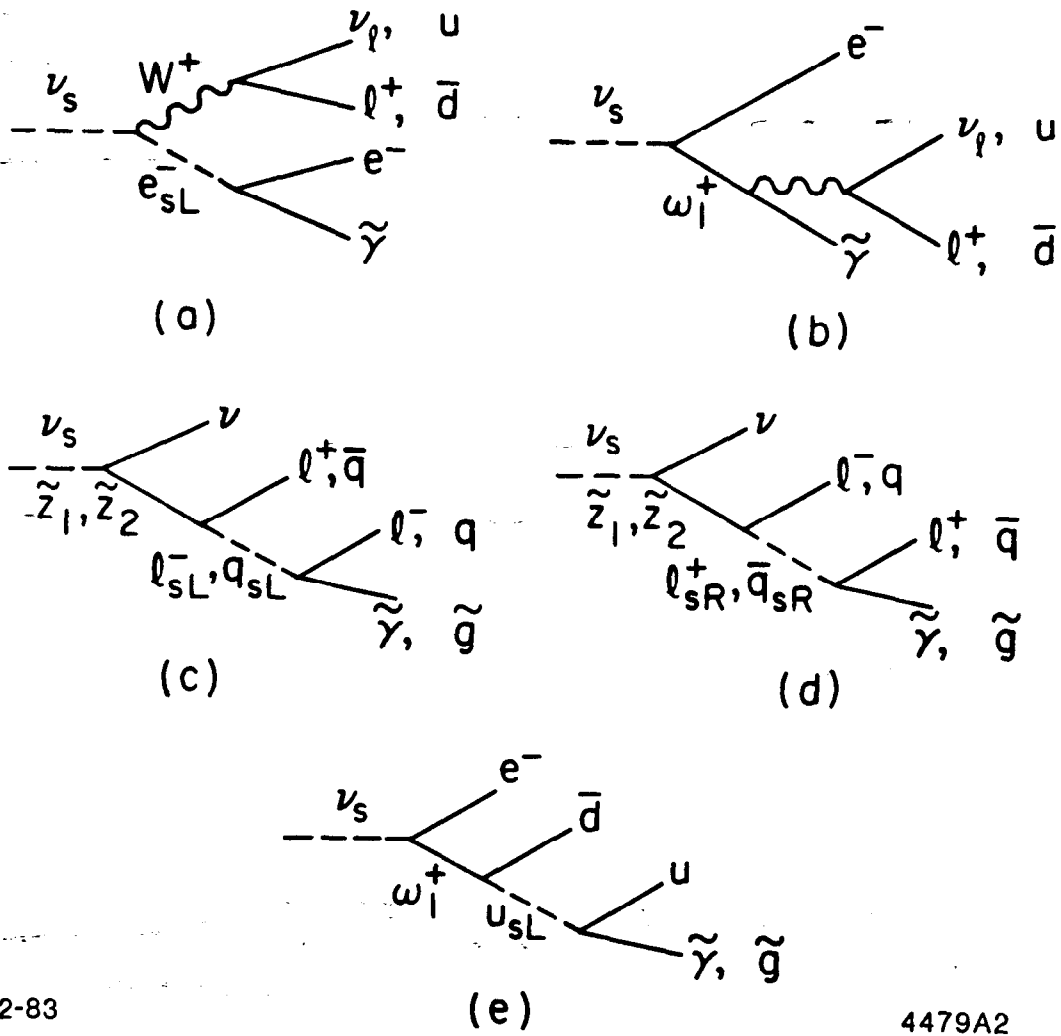
Fig. 1



7-83

4616A1

Fig. 2



2-83

4479A2

Fig. 3

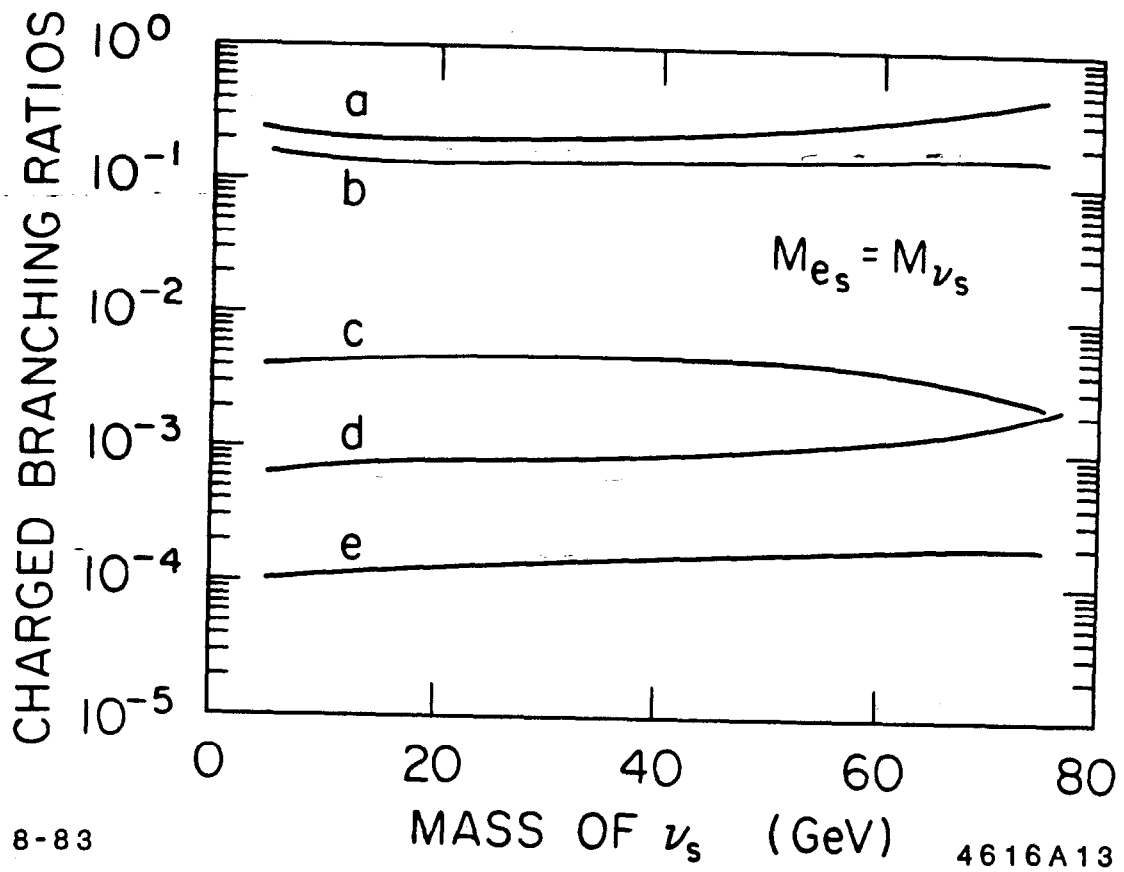


Fig. 4

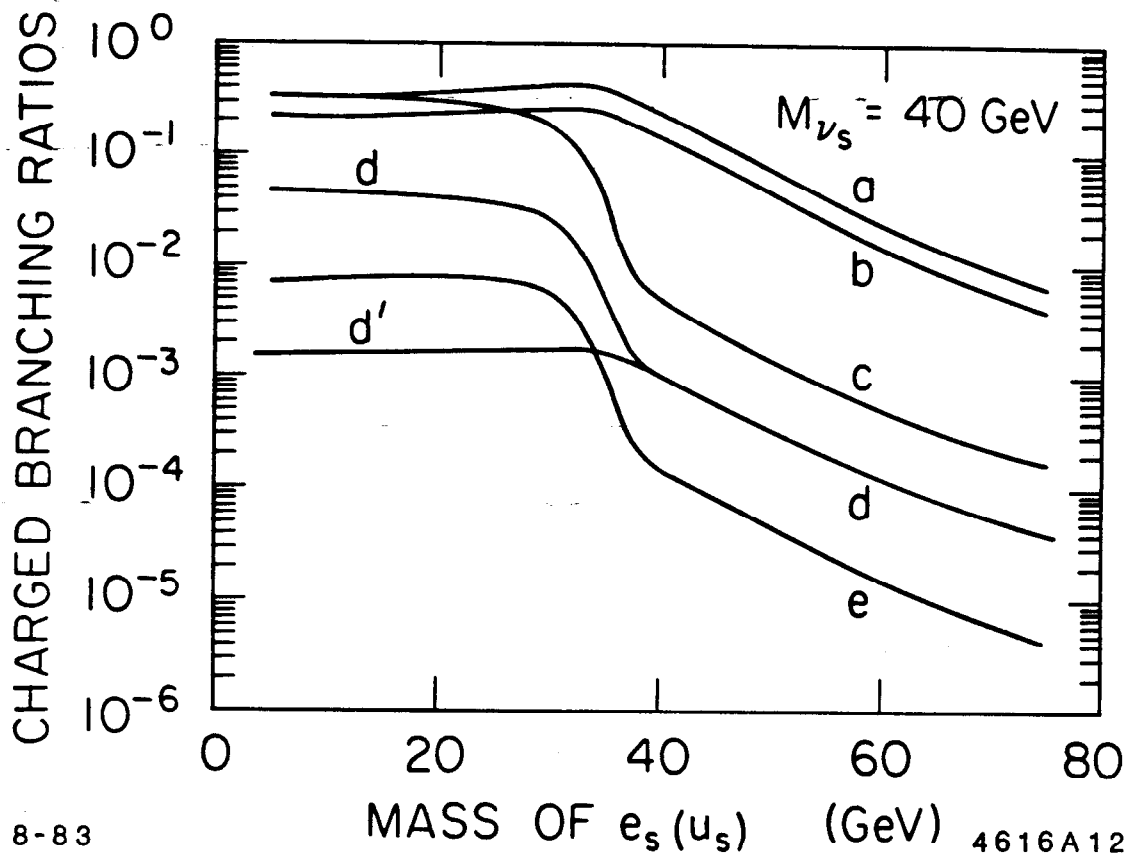
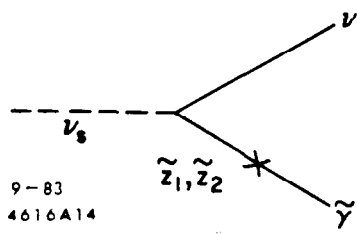
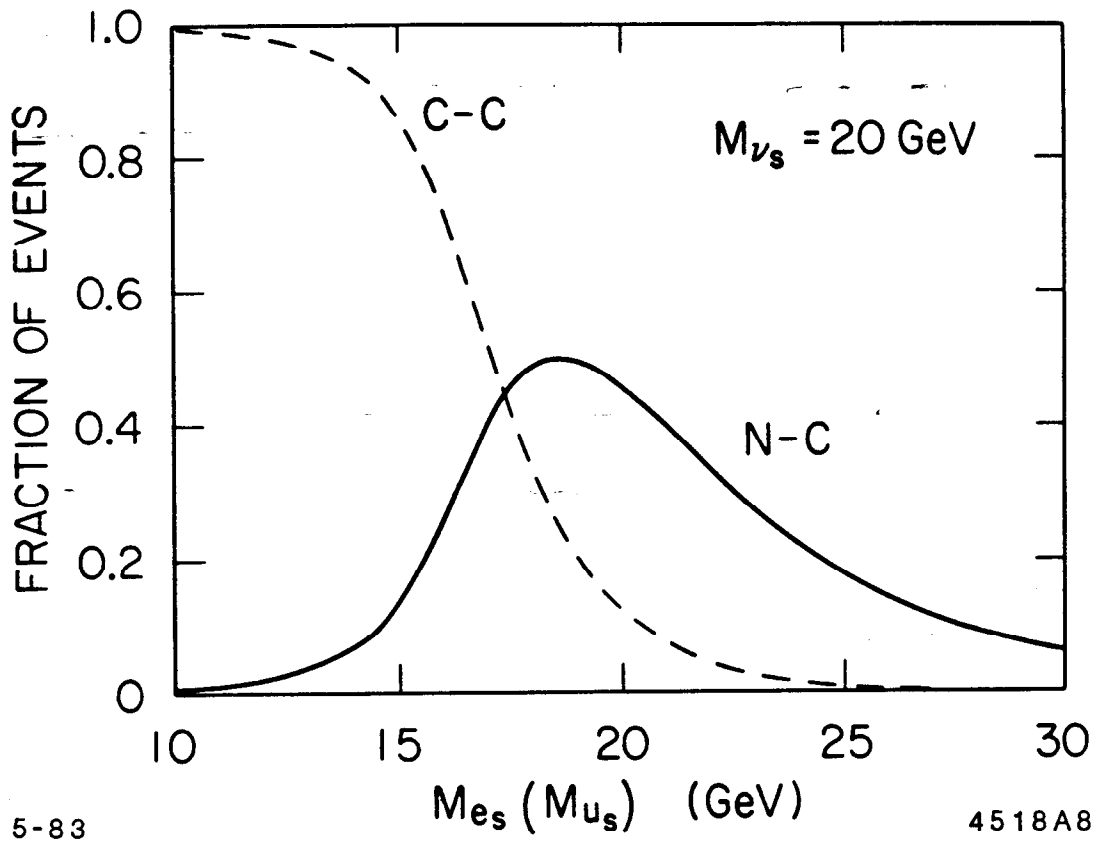


Fig. 5



9-83
4616A14

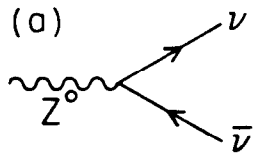
Fig. 6



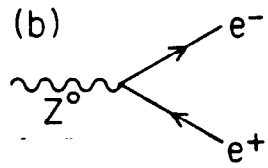
5-83

4518A8

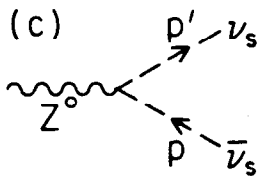
Fig. 7



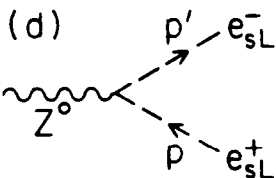
$$\frac{-ig}{4\cos\theta_W} \gamma^\mu (1-\gamma_5)$$



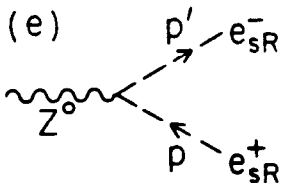
$$\frac{-ig}{4\cos\theta_W} \gamma^\mu [(\sin^2\theta_W - \cos^2\theta_W)(1-\gamma_5) + 2\sin^2\theta_W(1+\gamma_5)]$$



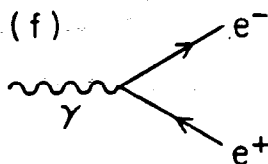
$$\frac{-ig}{2\cos\theta_W} (p+p')^\mu$$



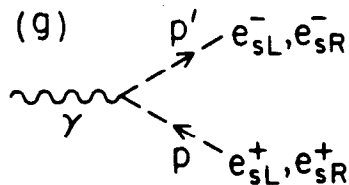
$$\frac{-ig}{2\cos\theta_W} (\sin^2\theta_W - \cos^2\theta_W) (p+p')^\mu$$



$$\frac{-ig \sin^2\theta_W}{\cos\theta_W} (p+p')^\mu$$

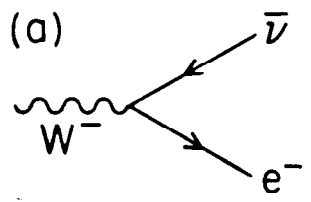


$$ie\gamma^\mu$$

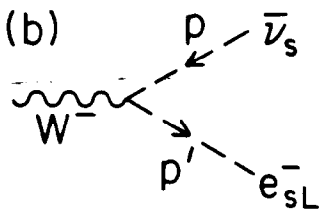


$$ie(p+p')^\mu$$

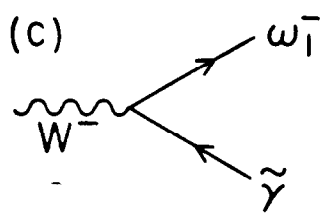
Fig. 8



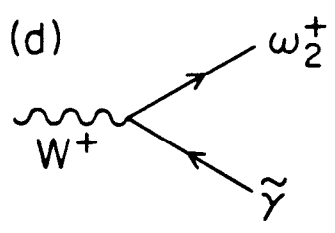
$$\frac{-ig}{2\sqrt{2}} \gamma^\mu (1-\gamma_5)$$



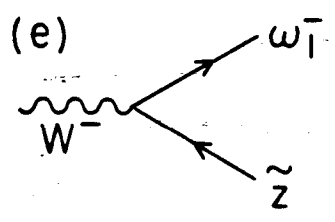
$$\frac{-ig}{\sqrt{2}} (p+p')^\mu$$



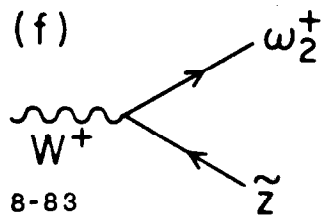
$$\frac{-ie}{2} \gamma^\mu (1+\gamma_5)$$



$$\frac{ie}{2} \gamma^\mu (1+\gamma_5)$$



$$\frac{-ig}{2} \left[\cos\theta_w \gamma^\mu (1+\gamma_5) + \frac{1}{2} \gamma^\mu (1-\gamma_5) \right]$$

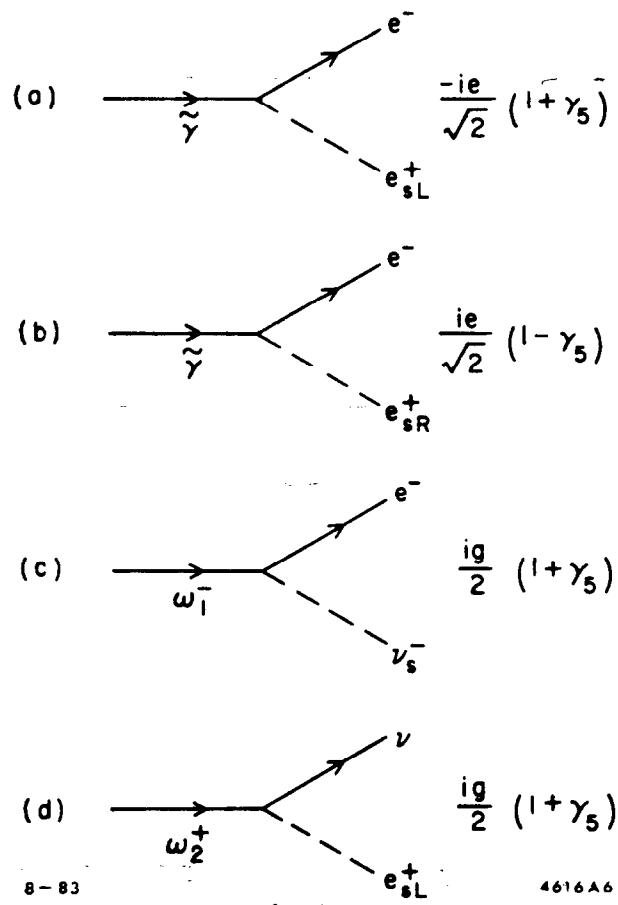


$$\frac{ig}{2} \left[\cos\theta_w \gamma^\mu (1+\gamma_5) + \frac{1}{2} \gamma^\mu (1-\gamma_5) \right]$$

8-83

4616A3

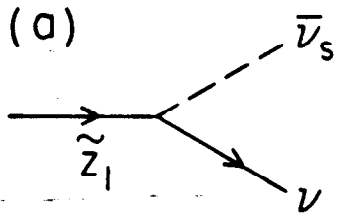
Fig. 9



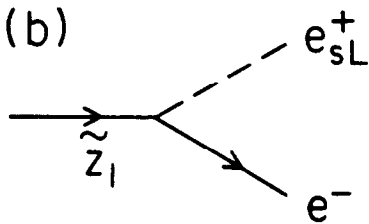
8-83

4616A6

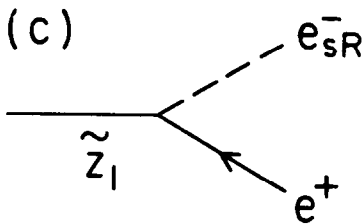
Fig. 10



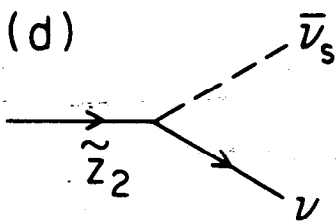
$$\frac{ig}{4\cos\theta_W} (1 + \gamma_5)$$



$$\frac{ig}{4\cos\theta_W} (\sin^2\theta_W - \cos^2\theta_W) (1 + \gamma_5)$$



$$\frac{-ig \sin^2\theta_W}{4\cos\theta_W} (1 + \gamma_5)$$

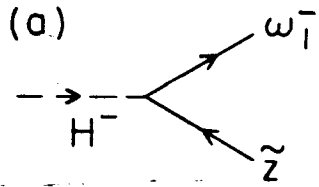


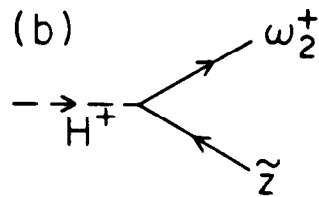
$$\frac{g}{4\cos\theta_W} (1 + \gamma_5)$$

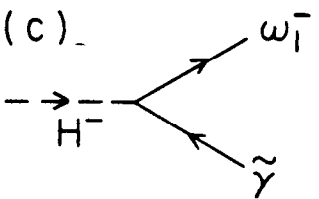
8-83

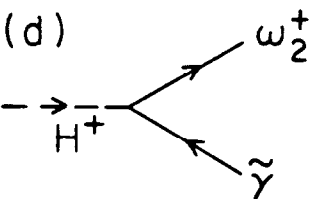
4616A7

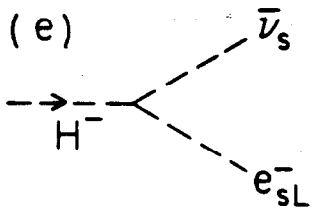
Fig. 11

(a)  $\frac{-ig}{4} \left[(1-\gamma_5) + \left(\frac{\cos^2\theta_W - \sin^2\theta_W}{\cos\theta_W} \right) (1+\gamma_5) \right]$

(b)  $\frac{ig}{4} \left[(1-\gamma_5) + \left(\frac{\cos^2\theta_W - \sin^2\theta_W}{\cos\theta_W} \right) (1+\gamma_5) \right]$

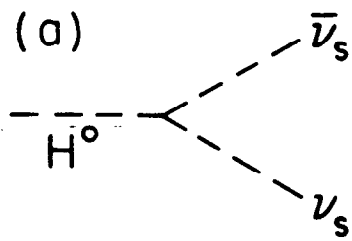
(c)  $\frac{-ie}{2} (1+\gamma_5)$

(d)  $\frac{ie}{2} (1+\gamma_5)$

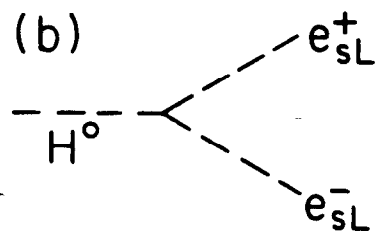
(e)  $\frac{igm_W}{\sqrt{2}}$

9-83
4616A4

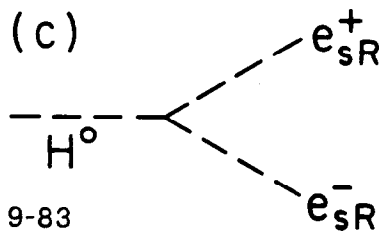
Fig. 12



$$\frac{igm_z}{2\cos\theta_w}$$



$$\frac{igm_z}{2\cos\theta_w} (\sin^2\theta_w - \cos^2\theta_w)$$



$$\frac{-igm_z \sin^2\theta_w}{\cos\theta_w}$$

9-83

4616A5

Fig. 13